

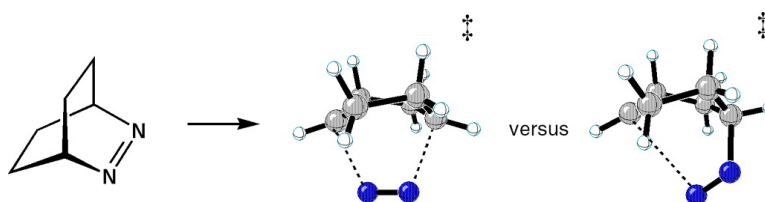
Article

One-Bond, Two-Bond, and Three-Bond Mechanisms in Thermal Deazetizations of 2,3-Diazabicyclo[2.2.2]oct-2-enes, *trans*-Azomethane, and 2,3-Diazabicyclo[2.2.1]hept-2-ene

Kelli S. Khuong, and K. N. Houk

J. Am. Chem. Soc., **2003**, 125 (48), 14867-14883 • DOI: 10.1021/ja038198l • Publication Date (Web): 11 November 2003

Downloaded from <http://pubs.acs.org> on March 30, 2009



More About This Article

Additional resources and features associated with this article are available within the HTML version:

- Supporting Information
- Links to the 1 articles that cite this article, as of the time of this article download
- Access to high resolution figures
- Links to articles and content related to this article
- Copyright permission to reproduce figures and/or text from this article

[View the Full Text HTML](#)

One-Bond, Two-Bond, and Three-Bond Mechanisms in Thermal Deazetizations of 2,3-Diazabicyclo[2.2.2]oct-2-enes, *trans*-Azomethane, and 2,3-Diazabicyclo[2.2.1]hept-2-ene

Kelli S. Khuong and K. N. Houk*

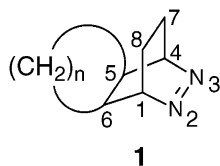
Contribution from the Department of Chemistry and Biochemistry, University of California, Los Angeles, California 90095-1569

Received August 28, 2003; E-mail: houk@chem.ucla.edu

Abstract: The thermal deazetizations of a series of substituted 2,3-diazabicyclo[2.2.2]oct-2-enes and some simpler model systems have been studied using the UB3LYP/6-31G(d) and CASPT2 methods, with a variety of active spaces. A fused cyclopropane exerts unique control on the mechanism and rate of deazetization. When the Walsh σ -orbitals are appropriately aligned in an exo orientation, a pericyclic three-bond cleavage occurs. For an endo-fused cyclopropane, sequential one-bond cleavages occur to take advantage of orbital overlap with the Walsh orbitals. In systems lacking strongly directing substituents, concerted two-bond cleavage pathways to form diradical intermediates have a small enthalpic advantage (ΔH_{0K}^\ddagger) over sequential one-bond cleavage pathways. However, the one-bond mechanism has an entropic advantage over the two-bond; consequently, at 400–500 K where decomposition occurs, one-bond and two-bond diradical cleavages both occur simultaneously. The thermal decompositions of *trans*-azomethane and 2,3-diazabicyclo[2.2.1]hept-2-ene are also studied, and the results are compared to extensive computational studies in the literature. Comparisons of UB3LYP, CASSCF, and CASPT2 surfaces for these reactions are made.

Introduction

The deazetization (nitrogen loss) of azoalkanes provides practical routes to radicals and diradicals and has elicited much mechanistic interest. Early concerns about one-bond versus two-bond cleavage of acyclic azoalkanes¹ have evolved into detailed explorations of the dynamics of deazetizations of cyclic and polycyclic azoalkanes.²



We report theoretical calculations with the density functional theory and complete active space SCF methods on deazetization mechanisms of a series of substituted 2,3-diazabicyclo[2.2.2]oct-2-enes (DBOs), **1**. These results show how substituent effects and stereoelectronics³ can alter the mechanism (Figure 1) from fully concerted (A), to two-bond stepwise with a diradical intermediate (B), to sequential one-bond cleavage leading first to a diazenyl diradical intermediate (C). The results establish the role of orbital overlap for cyclopropane and cyclobutane systems, as proposed long ago by Jorgensen.⁴

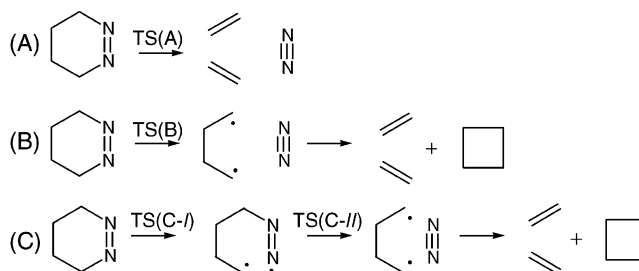


Figure 1. Three mechanisms for loss of N_2 from six-membered cyclic azoalkanes: three-, two-, and one-bond cleavage.

Activation parameters and relative rates for the thermal deazetization of DBO and its ring-fused derivatives vary substantially as a function of substitution ($\Delta H^\ddagger = 14\text{--}46$ kcal/mol).⁵ Table 1 gives the experimental activation parameters measured for the various DBOs studied here. Interpretations of the experimental kinetic data and product identities have led to the following conclusions. Compounds **2**, **4**, **5**, and **6** lose N_2 through a diradical process, the key diagnostics being the formation of diradical ring closure products for **2** and **6**, the

(1) Reviews: (a) Engel, P. S. *Chem. Rev.* **1980**, *80*, 99–150. (b) Meier, H.; Zeller, K.-P. *Angew. Chem., Int. Ed. Engl.* **1977**, *16*, 835–851.
 (2) Reyes, M. B.; Carpenter, B. K. *J. Am. Chem. Soc.* **2000**, *122*, 10163–10176 and references therein.
 (3) Berson, J. A. *Acc. Chem. Res.* **1991**, *24*, 215–222.
 (4) Jorgensen, W. L. *J. Am. Chem. Soc.* **1975**, *97*, 3082–3090.

(5) (a) Cohen, S. G.; Zand, R. J. *J. Am. Chem. Soc.* **1962**, *84*, 586–591. (b) Engel, P. S.; Hayes, R. A.; Kiefer, L.; Szilagy, S.; Timberlake, J. W. *J. Am. Chem. Soc.* **1978**, *100*, 1876–1883. (c) Allred, E. L.; Hinshaw, J. C. *J. Chem. Soc., Chem. Commun.* **1969**, 1021–1022. (d) Snyder, J. P.; Harpp, D. N. *J. Am. Chem. Soc.* **1976**, *98*, 7821–7823. (e) Allred, E. L.; Hinshaw, J. C. *Tetrahedron Lett.* **1972**, *5*, 387–388. (f) Engel, P. S.; Nalepa, C. J.; Horsey, D. W.; Keys, D. E.; Grow, R. T. *J. Am. Chem. Soc.* **1983**, *105*, 7102–7107. (g) Allred, E. L.; Voorhees, K. J. *J. Am. Chem. Soc.* **1973**, *95*, 620–621. (h) Martin, H.-D.; Heiser, B.; Kunze, M. *Angew. Chem., Int. Ed. Engl.* **1978**, *17*, 696–697.

Table 1. Experimental Kinetic Parameters for the Thermal Decomposition of DBO and Related Compounds

Azoalkane	E_a (kcal/mol)	ΔH^\ddagger (kcal/mol)	ΔS^\ddagger (e.u.)	Temp (°C)	ref
2	44.6 ± 0.2	43.6 ± 0.2 [a]	10.5 ± 0.3	199.5-259.0	5a
	46.0 ± 0.2 [a]	45.0 ± 0.2	10.6 ± 0.4	230.2-256.0	5b
3	14.9 ± 1.5	14.3 ± 1.5 [a]	-21	-3.5-12.0	5c
	22.1 ± 0.4	21.5 ± 0.4 [a]	4.1 ± 1.1	25	5d
4	46.9 ± 2.0 [a]	45.9 ± 2.0	10.4 ± 3.8	240	5f
5	41.4 ± 0.3	40.5 ± 0.3 [a]	10.3	176.9-199.2	5g
6	39.2 ± 0.3	38.3 ± 0.3 [a]	11	150.2-175.3	5c
					5e
					5h
7	N.A.	N.A.	N.A.		
8 AM	51.2 ± 0.3	50.1 ± 0.3 [a]	10.0 ± 0.7	290	7a
	55.4 ± 0.6	54.4 ± 0.6 [a]	17.4 ± 1.0	254.1-294.0	7b
	51.2	50.1 [a]	14.1	278.6-327.4	7c
	52.5	51.3 [a]	13.6	292-336	7d
	50.2	49.1 [a]	10.9	290, 310	7e
9 DBH	37.3 ± 0.3	36.5 ± 0.3 [a]	8.7 ± 0.4	131.5-180.8	8a
	36.9 ± 0.2	36.0 ± 0.2 [a]	5.8 ± 0.5	171.0-202.4	8b

^a Calculated using the relationship $E_a = \Delta H^\ddagger + nRT$, where $n = 1$ for a unimolecular reaction and T is taken as the average temperature.

relatively consistent activation enthalpies ($\Delta H^\ddagger = 38$ – 46 kcal/mol, Table 1), and the positive values of ΔS^\ddagger . Compound **3** loses N_2 through a pericyclic [2+2+2] cycloreversion as evidenced by the significantly lower ΔH^\ddagger and more negative ΔS^\ddagger .⁶ Compound **7** is the only member of this series that has not been studied experimentally. Azomethane⁷ (**8**) and 2,3-diazabicyclo[2.2.1]hept-2-ene⁸ (**9**) are included for comparison and are discussed later.

Whereas **3** exhibits unique activation parameters, the remaining experimentally determined activation parameters fail to distinguish between one-bond and two-bond cleavage mechanisms in the DBO series. In an effort to understand how a fused-cyclopropane or fused-cyclobutane influences the preference for three-, two-, or one-bond cleavage, we have fully characterized mechanisms A–C for DBO compounds **2**–**7** with several levels of theory. We also provide a literature survey and our computational results on *trans*-azomethane (**AM**) and the smaller bicyclic analogue **DBH**, **9**.

Results and Discussion

Transition structures were fully optimized with RB3LYP/6-31G(d) or UB3LYP/6-31G(d) using Gaussian 98.⁹ All stationary points were characterized by frequency calculations. Intrinsic reaction coordinate (IRC) calculations were used to confirm pericyclic transition structures **2-TS(A)** and **6-TS(A)** and diradical transition structures **6-TS(B)**, **2-TS(C-Ia)**, **3-TS(C-I)**, **5-TS(C-I)**, and **7-TS(C-I)**. The $\langle S^2 \rangle$ values for TS(B) range from 0.55 to 0.70, and the $\langle S^2 \rangle$ values for TS(C-I) range from 0.88 to 0.95. Spin corrections were not made. For the DBO parent, **2**, the bicyclo[2.2.1] analogue, **9**, and *trans*-azomethane, full optimizations of the diradical structures were performed at the CASSCF/6-31G(d) level with various active spaces.¹⁰

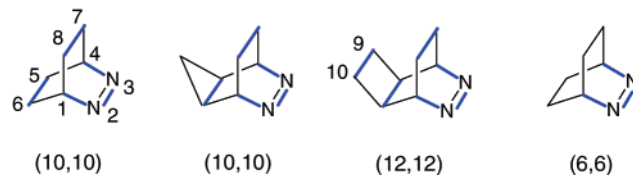


Figure 2. Bonds highlighted in blue indicate the bonding and antibonding orbitals included in the active space of the CASPT2/6-31G(d)/(U)B3LYP/6-31G(d) single point calculations.

CASPT2/6-31G(d)/(U)B3LYP/6-31G(d) single point energies were calculated using MOLCAS.¹¹ A (10,10) active space was used for the calculations on the DBO parent and cyclopropane

(6) Related cyclopropane-fused systems: (a) Allred, E. L.; Hinshaw, J. C.; Johnson, A. L. *J. Am. Chem. Soc.* **1969**, *91*, 3382–3383. (b) Berson, J. A.; Olin, S. S. *J. Am. Chem. Soc.* **1969**, *91*, 777–778.

(7) Note that log A values have been converted to ΔS^\ddagger values. (a) Steel, C.; Trotman-Dickenson, A. F. *J. Chem. Soc.* **1959**, 975 [log $A = 15.7 \pm 0.15$, $T = 554$ K]. (b) Forst, W.; Rice, O. K. *Can. J. Chem.* **1963**, *41*, 562 [log $A = 17.3 \pm 0.23$, $T_{\text{avg}} = 526.5$ K]. (c) Ramsperger, H. C. *J. Am. Chem. Soc.* **1927**, *49*, 912 [data recalculated in ref d; log $A = 16.6$, $T_{\text{avg}} = 577.4$ K]. (d) Taylor, H. A.; Jahn, F. P. *J. Chem. Phys.* **1939**, *7*, 470 [log $A = 16.5$, $T_{\text{avg}} = 597.2$ K]. (e) Rice, O. K.; Sickman, D. V. *J. Chem. Phys.* **1936**, *4*, 242 [log $A = 15.9$, $T_{\text{avg}} = 572$ K].

(8) (a) Cohen, S. G.; Zand, R.; Steel, C. *J. Am. Chem. Soc.* **1961**, *83*, 2895–2900. (b) Crawford, R. J.; Mishra, A. *J. Am. Chem. Soc.* **1966**, *88*, 3963–3969.

Table 2. Calculated Activation Enthalpies ($\Delta H_{\text{OK}}^\ddagger$, kcal/mol) and Activation Entropies ($\Delta S_{298\text{K}}^\ddagger$, eu) for mechanisms A–C

DBO	TS (A): three-bond			TS (B): two-bond			TS (C-I): one-bond, first			TS (C-II): one-bond, second		
	CASPT2 ^a		RB3LYP	CASPT2	UB3LYP		CASPT2	UB3LYP		CASPT2	UB3LYP	
	ΔH^\ddagger	ΔH^\ddagger	ΔS^\ddagger	ΔH^\ddagger	ΔH^\ddagger	ΔS^\ddagger	ΔH^\ddagger	ΔH^\ddagger	ΔS^\ddagger	ΔH^\ddagger	ΔH^\ddagger	ΔS^\ddagger
2	44.4	50.1 ^b	9.6	41.0	40.6	9.4	40.5	39.5	6.6	42.3	38.0	14.4
							41.5	40.1	9.3	37.7	34.8	11.2
3	20.9	17.9	4.2		<i>e</i>		33.7	31.5	7.2	33.8	29.2	12.6
4		<i>c</i>		42.0	41.1 ^f	4.3	37.8	37.1	4.2	36.0	31.6	11.8
5	43.3	40.8 ^d	6.0	36.2	35.9	8.0	34.3	33.5	5.4	33.7	28.5	12.5
6	38.0	37.5	4.0	34.2	34.7	5.2	35.5	34.8	3.3	37.4	33.3	10.5
7	46.9	48.9 ^b	9.0	41.4	40.0	10.0	41.7	39.3	9.1	40.1	36.6	11.2

^a CASPT2/6-31G(d)//(U)B3LYP/6-31G(d); CASPT2//CASSCF energies with various active spaces are included in the text. ^b RHF to UHF wave function instability. ^c A [2+2+2] cycloreversion transition structure cannot be located. See text for details. ^d The [2+2+2] transition structure involves cleavage of the exo-cyclobutane σ -bond, not the endo-cyclopropane σ -bond. ^e A two-bond diradical cleavage transition structure cannot be located. Stretching both C–N bonds leads to a [2+2+2] pathway instead. See text for details. ^f A second-order saddle point.

derivatives; the active space included the C1–N2, C4–N3, C5–C6, and C7–C8 σ/σ^* orbitals and the N=N π/π^* orbitals (Figure 2). A (12,12) active space was used for the cyclobutane derivatives because in some cases the C9–C10 bond could not be excluded from the active space. The (U)B3LYP zero-point energies and thermodynamic functions were used to correct the CASPT2 electronic energies.

(6,6)CASPT2/6-31G(d)//(U)B3LYP/6-31G(d) single points were carried out for the parent, endo-cyclopropane, and endo-cyclobutane systems. Increasing the size of the active space from (6,6) to (10,10) or (12,12) caused the relative energies of the diradical transition structures and intermediates to decrease by 0.1–0.3 kcal/mol. The energy differences between the one-bond cleavage and the two-bond cleavage pathways were unchanged, indicating that the diradical loss of N₂ can be adequately described by the smaller (6,6) active space including the C1–N2, C4–N3 σ/σ^* orbitals and the N₂=N₃ π/π^* orbitals (Figure 2). The (6,6)CASPT2// (U)B3LYP energies are included in the Supporting Information.

The (U)B3LYP and CASPT2 activation enthalpies at 0 K (electronic energies plus (U)B3LYP ZPEs) and (U)B3LYP activation entropies at 298 K are all summarized in Table 2. The initial discussion will focus on the ΔH surfaces at 0 K, facilitating direct comparison of the activation barriers among the DBO series. Later in the discussion, we will address the role of entropy by comparing the calculated activation parameters at the average experimental temperature to the experimental activation parameters for each of the DBOs.

- (9) Frisch, M. J.; Trucks, G. W.; Schlegel, H. B.; Scuseria, G. E.; Robb, M. A.; Cheeseman, J. R.; Zakrzewski, V. G.; Montgomery, J. A., Jr.; Stratmann, R. E.; Burant, J. C.; Dapprich, S.; Millam, J. M.; Daniels, A. D.; Kudin, K. N.; Strain, M. C.; Farkas, O.; Tomasi, J.; Barone, V.; Cossi, M.; Cammi, R.; Mennucci, B.; Pomelli, C.; Adamo, C.; Clifford, S.; Ochterski, J.; Petersson, G. A.; Ayala, P. Y.; Cui, Q.; Morokuma, K.; Malick, D. K.; Rabuck, A. D.; Raghavachari, K.; Foresman, J. B.; Cioslowski, J.; Ortiz, J. V.; Baboul, A. G.; Stefanov, B. B.; Liu, G.; Liashenko, A.; Piskorz, P.; Komaromi, I.; Gomperts, R.; Martin, R. L.; Fox, D. J.; Keith, T.; Al-Laham, M. A.; Peng, C. Y.; Nanayakkara, A.; Challacombe, M.; Gill, P. M. W.; Johnson, B.; Chen, W.; Wong, M. W.; Andres, J. L.; Gonzalez, C.; Head-Gordon, M.; Replogle, E. S.; Pople, J. A. *Gaussian 98*, revision A.9; Gaussian, Inc.: Pittsburgh, PA, 1998.
- (10) CASSCF/6-31G(d) optimizations were performed with (4,4), (6,6), and (10,8) active spaces such that the (4,4) active space included both sets of C–N σ/σ^* orbitals, the (6,6) active space added in the N=N π/π^* orbitals, and the (10,8) active space added in the nitrogen lone pairs. Note that the (4,4) active space in ref 2 included one set of C–N σ/σ^* orbitals and the N=N π/π^* orbitals.
- (11) Andersson, K.; Barysz, M.; Bernhardsson, A.; Blomberg, M. R. A.; Cooper, D. L.; Fleig, T.; Fülischer, M. P.; de Graaf, C.; Hess, B. A.; Karlström, G.; Lindh, R.; Malmqvist, P.-Å.; Neogrády, P.; Olsen, J.; Roos, B. O.; Sadlej, A. J.; Schimmelpfennig, B.; Schütz, M.; Seijo, L.; Serrano-Andrés, L.; Siegbahn, P. E. M.; Ståhring, J.; Thorsteinsson, T.; Veryazov, V.; Widmark, P.-O. *MOLCAS*, Version 5.0; Lund University: Sweden, 2001.

The Parent 2,3-Diazabicyclo[2.2.2]oct-2-ene (2). As shown in Table 2, the parent DBO **2** clearly has a preference for decomposition via diradical intermediates. The pericyclic three-bond cleavage requires ~ 3 kcal/mol more energy than the possible diradical pathways. The restricted B3LYP wave function for **2**-TS(A) is unstable, indicating that an unrestricted wave function would provide a better description of the electronic structure at this geometry. These observations also apply to **7**-TS(A), and the pericyclic loss of N₂ from compound **7** is also expected to be inoperative.

The key stationary points in the diradical decomposition pathways for **2** are illustrated in Figure 3. In this and subsequent figures, both CASPT2 and (U)B3LYP energies of the (U)-B3LYP optimized structures are shown, and the structures in the diagram are presented in order according to the CASPT2 energies. Figure 3 has two prominent features: (1) the UB3LYP and CASPT2 results predict that two-bond cleavage and one-bond cleavage are competitive with activation enthalpies within 1 kcal/mol of each other, and (2) there are two possible modes of cleaving the C1–N2 σ bond, such that one mode involves a twist-boat geometry of the cyclohexane moiety while the other involves a chair geometry.

Transition structure **2**-TS(B) has an enthalpy of 41.0 kcal/mol and leads to direct formation of the twist-boat 1,4-cyclohexane diyl and a molecule of N₂. The 1,4-diyl is the common intermediate for formation of either 1,5-hexadiene or bicyclobutane. Hrovat and Borden recently reported a thorough (6,6)CASPT2// (6,6)CASSCF study of the bicyclo[2.2.0]hexane/1,5-hexadiene rearrangement, focusing much attention on the 1,4-cyclohexane diyl.¹²

Transition structure **2**-TS(C-Ia) has an enthalpy of 40.5 kcal/mol relative to reactant. It leads to the formation of a cyclohexyldiazanyl diradical in which the carbon framework adopts a twist-boat conformation. The diazenyl diradical defines a very flat region of the potential energy surface, in which the pendant diazenyl group can adopt several rotational conformations¹³ which lie within 0.4 kcal/mol of each other; only one conformer, the one initially formed from bond cleavage, is shown for clarity. Minimal stretching of the second C–N bond leads to loss of N₂ and formation of the twist-boat 1,4-diyl via transition structure **2**-TS(C-IIa). Again, several transition structures differing only in the rotational conformation of the diazenyl group

- (12) Hrovat, D. A.; Borden, W. T. *J. Am. Chem. Soc.* **2001**, *123*, 4069–4072.
- (13) Nearly degenerate rotational conformers in a diazenyl diradical were first computed for **DBH** in ref 26.

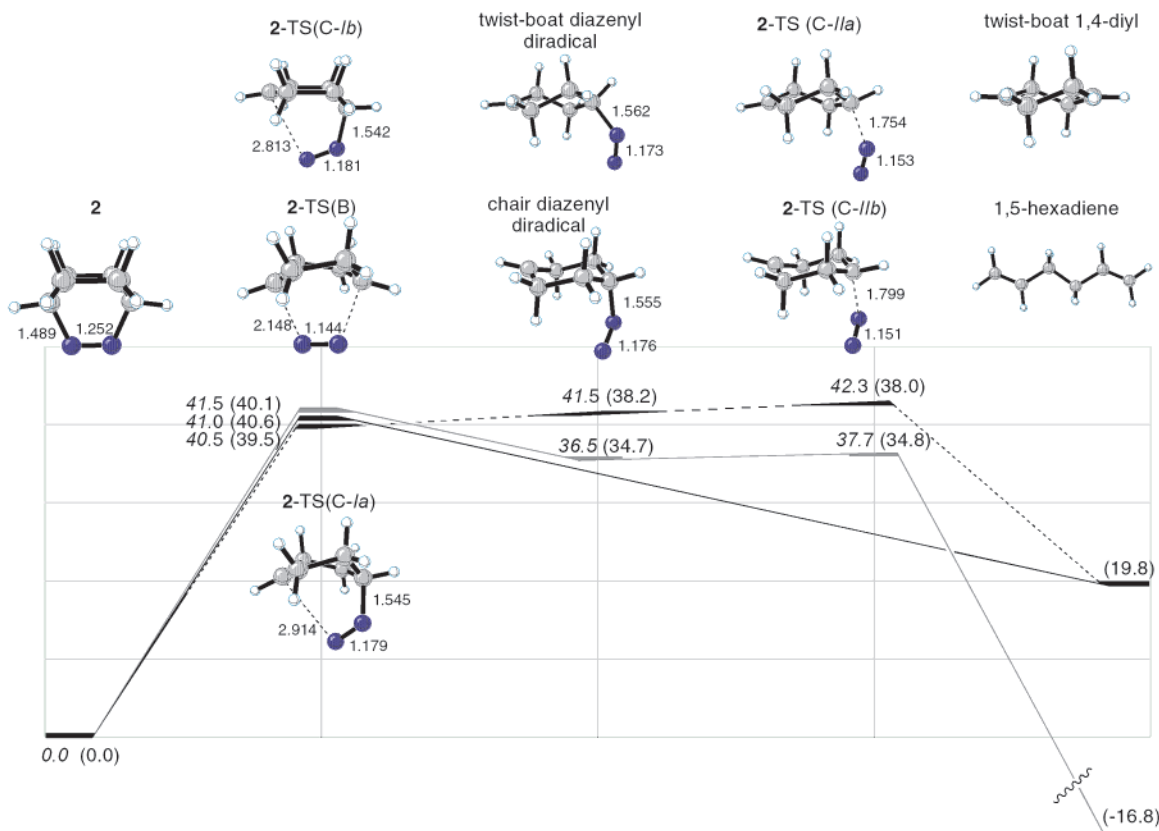


Figure 3. Deazetization of **2** by mechanisms B and C. ΔH_{0K}^{\ddagger} values are in kcal/mol and correspond to (10,10)CASPT2 single points and (R and UB3LYP/6-31G* optimizations). Bond lengths are in Å.

lie within 0.6 kcal/mol of each other, and only the one corresponding to the same geometry as the diazenyl diradical precursor is shown. For this sequential bond cleavage pathway, the cleavage of the second C–N bond, TS(C-IIa), is the rate-limiting step according to the CASPT2 calculations.

Transition structure 2-TS(C-Ib) is slightly higher in energy than 2-TS(C-Ia) and leads to the formation of the chairlike diazenyl diradical. The chair cyclohexyl-diazenyl diradical is 5 kcal/mol more stable than the twist-boat analogue. Cleavage of the second C–N bond leads to the formation of N₂ plus 1,5-hexadiene because the incipient chair 1,4-cyclohexane diyl is not a local minimum on the potential energy surface.

One striking feature of the DBO potential energy surface is that TS(C-Ia) and TS(C-Ib) are true transition structures on the UB3LYP potential energy surface: there is a barrier on the potential energy surface for the twist-boat or chairlike diazenyl diradical to collapse back to reactant. This differs from the behavior of *trans*-azomethane **AM**¹⁴ and the extensively studied bicyclo[2.2.1] analogue **DBH**, described in more detail later.² In the case of **AM** or **DBH**, stretching one C–N bond leads to a Morse-like potential energy profile in which no maximum can be identified as a true transition structure.

The cyclohexane framework of compound **2** is the structural feature that is responsible for this unique behavior. For both

transition structures 2-TS(C-Ia) and 2-TS(C-Ib), the stretching of the C–N is accompanied by a well-defined conformational change of the 6-carbon ring from a boat to a twist-boat (in the case of *a*) or to a chair (*b*). The combination of these two vibrations, the C–N stretch and the conformational flip, leads to the presence of a maximum on the UB3LYP potential energy surface, and, consequently, there is a barrier for the cyclohexyl-diazenyl diradical to collapse back to the closed-shell reactant.

A comparison of CASPT2 and UB3LYP results is an important aspect of this work, and the results from the methods are compared throughout this paper. For the parent DBO **2**, and for the remaining DBO systems, the CASPT2 and UB3LYP relative enthalpies of diradical transition structures TS(B) and TS(C-I) are in excellent agreement. On the other hand, CASPT2 systematically predicts that diazenyl diradicals are 3–4 kcal/mol higher in enthalpy than predicted by UB3LYP. Also, CASPT2 predicts that cleavage of the second C–N bond, TS(C-II), has a 1 kcal/mol barrier, while UB3LYP predicts no barrier for the second C–N bond cleavage once ZPE is included. Similar trends can be observed for all of the diradical pathways presented in this paper. In general, when the CASPT2 and UB3LYP results differ significantly, we take the CASPT2 energies to be more reliable. A more complete analysis of the CASPT2 and UB3LYP results is presented at the end of the Results and Discussion section.

Obviously, CASPT2/UB3LYP methodology is highly dependent on the ability of B3LYP to provide accurate geometries for both closed-shell and open-shell singlet species. Because CASSCF is another common methodology for studying singlet diradicals, we wanted to verify the stationary points TS(B), TS-

(14) (a) Liu, R.; Cui, Q.; Dunn, K. M.; Morokuma, K. *J. Chem. Phys.* **1996**, *105*, 2333–2345. (b) Hon, N. W. C.; Chen, Z.-D.; Liu, Z.-F. *J. Phys. Chem. A* **2002**, *106*, 6792–6801. (c) Hu, C.-H.; Schaefer, H. F., III. *J. Phys. Chem.* **1995**, *99*, 7057–7513. (d) Hu, C.-H.; Schaefer, H. F., III. *J. Chem. Phys.* **1994**, *101*, 1289–1292. (e) Andrews, B. K.; Weisman, R. B. *J. Chem. Phys.* **1994**, *101*, 6776–6781. (f) Diau, E. W.-G.; Abou-Zied, O. K.; Scala, A. A.; Zewail, A. H. *J. Am. Chem. Soc.* **1998**, *120*, 3245–3246. (g) Vrābel, I.; Biskupič, S.; Staško, A. *J. Phys. Chem. A* **1997**, *101*, 5805–5812.

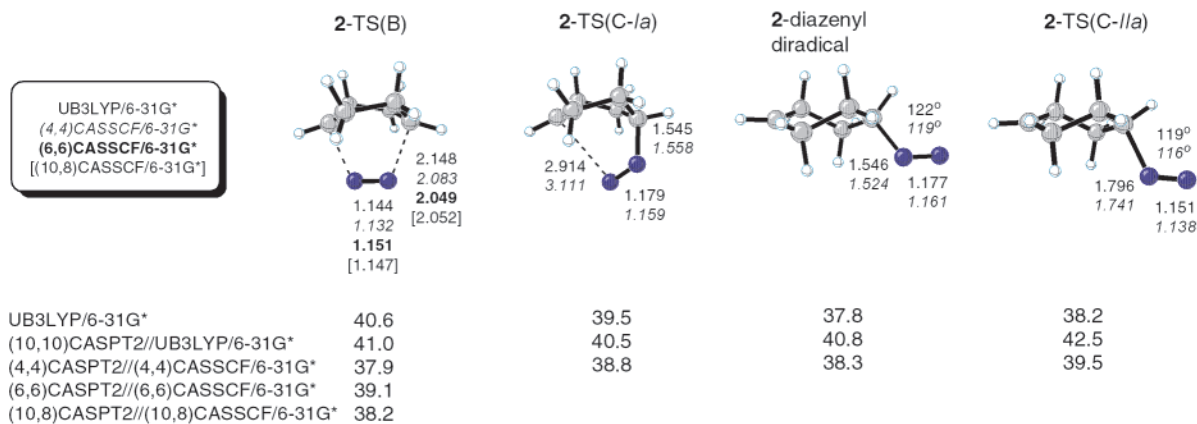


Figure 4. Diradical transition structures and intermediates optimized using UB3LYP, (4,4)CASSCF,¹⁰ (6,6)CASSCF, and (10,8)CASSCF. Bond lengths are given in Å. Relative ΔH_{0K}^{\ddagger} values are given in kcal/mol.

(C-Ia), the twist-boat diazenyl diradical, and TS(C-IIa) with CASSCF. Full CASSCF/6-31G(d) optimizations were performed with (4,4), (6,6), and (10,8) active spaces such that the (4,4) active space included both sets of C–N σ/σ^* orbitals, the (6,6) active space added in the N=N π/π^* orbitals, and the (10,8) active space added in the nitrogen lone pairs.¹⁰ Figure 4 summarizes these results. The two-bond cleavage TS, 2-TS(B), could be optimized regardless of the active space. On the other hand, the stationary points along the one-bond cleavage pathway¹⁵ could only be optimized using the (4,4) active space. With the larger active spaces, searches for 2-TS(C-Ia) led only back to 2-TS(B), while the searches for either the cyclohexyl-diazenyl diradical or 2-TS(C-IIa) led only to N₂ and cyclohexane diyl.

Further insight into these discrepancies was obtained by studying the cyclohexyl-diazenyl diradical system. The conversion of the diazenyl diradical to cyclohexane-diyl plus N₂ can be adequately defined by a single coordinate: the length of the C–N bond. Scans of that distance, shown in Figure 5, reveal that UB3LYP and (4,4)CASSCF predict a barrier to cleavage of the C–N bond, whereas (6,6)CASSCF and (10,8)CASSCF predict the absence of such a barrier (Figure 5, filled points). CASPT2 single points were also carried out for various C–N bond lengths along the scan (Figure 5, open points). The CASPT2 single points predict that a barrier is present regardless of the active space and that the transition structure for cleavage has a longer C–N bond length than predicted by either CASSCF or UB3LYP. On the basis of these findings, the following conclusions are made: (1) for these systems, UB3LYP provides optimized geometries most similar to (4,4)CASSCF, (2) the location of stationary points with CASSCF is highly dependent on the choice of active space, and the larger active spaces are not guaranteed to be more accurate, and (3) UB3LYP surface shape resembles the CASPT2 surface shape and appears to be an efficient computational method for locating singlet diradical stationary points involved in the loss of N₂ from DBOs. Presumably, one problem with the larger CASSCF active spaces stems from unbalanced representation of the diazenyl diradical and the cyclohexane-diyl plus N₂ electronic structures, resulting

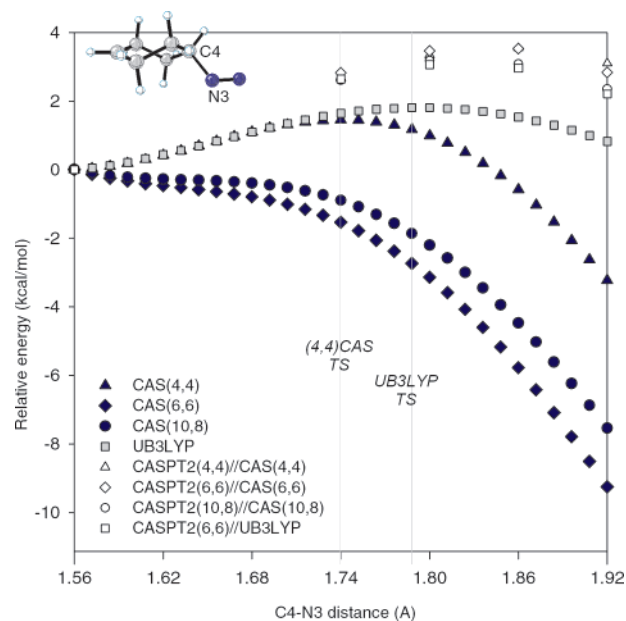


Figure 5. Change in the relative energy (ZPE exclusive) of the cyclohexyl-diazenyl diradical as the C4–N3 bond distance is increased from 1.56 to 1.92 Å.

from uneven neglect of dynamical correlation energy. A recent study on the photochemical decomposition of DBH also reported similar discrepancies between the CASSCF and CASPT2//CASSCF surfaces in which a (12,10) active space was used and showed that better agreement with CASPT2//CASSCF could be obtained with UB3LYP.¹⁶

On the basis of the CASPT2//UB3LYP results (Table 2, Figure 3), the parent DBO **2** has a slight preference for decomposition by a two-bond mechanism. Although this conclusion is preliminary because the effects of entropy and elevated experimental temperatures still need to be addressed (see below), the potential energy surface for decomposition of **2** will serve as a reference point for the remaining compounds in the DBO series.

Cyclopropane-Fused Derivatives. Computations agree with experimental observations that compound **3**, the exo-cyclopropane-fused DBO, decomposes by a facile concerted [2+2+2] cycloreversion (Figure 6). The key structural feature is the Walsh

(15) When diazenyl diradicals were optimized or scanned with both CASSCF and UB3LYP (see Figures 4, 5, 19, 20), the *exo* conformation of the diazenyl group was chosen because the rotational preference of the diazenyl group was defined clearly as being eclipsed with the C4–H bond.

(16) Sinicropi, A.; Page, C. S.; Adam, W.; Olivucci, M. *J. Am. Chem. Soc.* **2003**, *125*, 10947–10959.

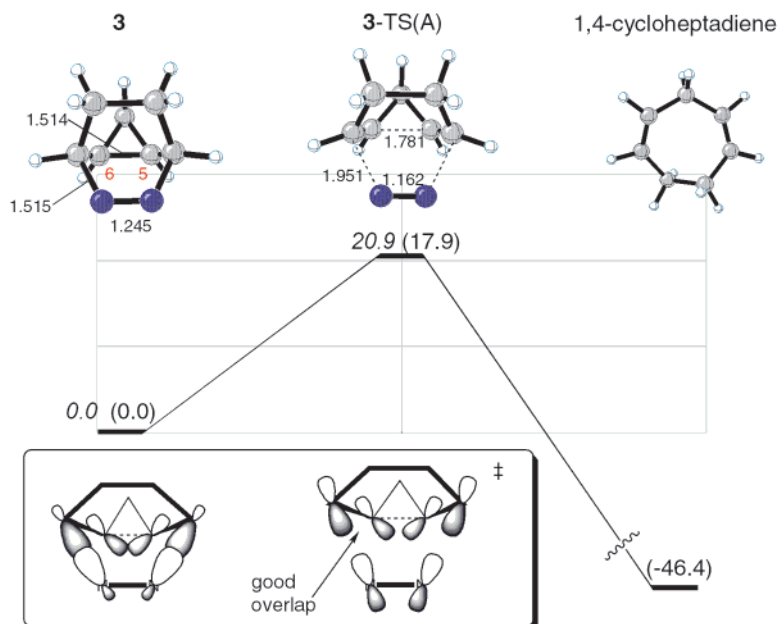


Figure 6. Deazetization of **3** by mechanism A. The bent-bond orbitals of the cyclopropane overlap nearly perfectly with the breaking C–N bonds in the [2+2+2] cycloreversion transition structure. ΔH_{0K}^\ddagger values are in kcal/mol and correspond to (10,10)CASPT2 single points and (RB3LYP/6-31G* optimizations). Bond lengths are in Å.

type orbitals of the exo-cyclopropane, noted earlier by Jorgensen,⁴ Allred,^{5c,6a} and Berson.^{6b} The C5–C6 σ bond has significant bent-bond character and is properly aligned to maximize cyclic orbital overlap of the cyclopropane Walsh orbitals and the breaking C–N σ bonds. As a result of this dramatic preorganization, the transition structure **3-TS(A)** is early and relatively low in energy.

Neither the two-bond nor the one-bond diradical pathway is competitive with the three-bond pericyclic pathway. In fact, a transition structure for the simultaneous stretching of two C–N bonds, **3-TS(B)**, cannot be optimized because the fused cyclopropane bond automatically cleaves. It is noteworthy that the one-bond cleavage transition structure, **3-TS(C-I)**, is relatively low in energy as compared to the TS(C-I) energies for the rest of the DBO series, but it is still 12.8 kcal/mol (CASPT2) higher in energy than the pericyclic cleavage transition structure.

Both compounds **4** and **5** contain an endo-fused cyclopropane, and as for compound **3**, it is the stereoelectronic effect of the cyclopropane that dominates the relative enthalpies of mechanisms A, B, and C. However, in **4** and **5**, the Walsh orbitals of the endo-cyclopropane are essentially orthogonal to the C–N σ bonds; consequently, the stabilizing effect of cyclic orbital overlap is completely absent, making the pericyclic TS(A) inaccessible for **4** and prohibitively high in energy for **5**. Likewise, the endo-cyclopropane affords no extra stabilization to the two-bond homolysis of mechanism B. Alternatively, mechanism C can take advantage of the bent-bond character of the C5–C6 σ bond. The calculated ΔH_{0K}^\ddagger values for **4-TS(C-I)** and **5-TS(C-I)** are 37.8 and 34.3 kcal/mol, respectively. The motion associated with the one-bond cleavage aligns the forming C1 radical into a favorable cyclopropylcarbiny geometry (Figures 7 and 8). Shortening of the C1–C6 bond relative to the C4–C5 bond in **4-TS(C-I)** and **5-TS(C-I)** is a measure of the two-orbital, three-electron stabilizing interactions between the C1 radical and the endo-cyclopropane Walsh orbitals.

As shown in Figure 7, **4-TS(C-I)** leads to the formation of a diazenyl diradical, with radical centers located at C1 and N2.

Again, the diazenyl group is now free to rotate about the N3–C4 bond and can adopt one of three possible conformations that differ in energy by only ± 0.5 kcal/mol. Each conformation of the diazenyl diradical leads to a unique conformation for cleavage of the second C–N bond, and these transition structures fall within ± 0.4 kcal/mol of each other. Cleavage of the second C–N bond leads directly to the formation of product, because the 1,4-singlet diradical is not a local minimum. A very similar potential energy surface is calculated for compound **5**, the endo-cyclopropane-exo-cyclobutane DBO (Figure 8). The main difference is that the one-bond pathway for compound **5** is lower in energy than the one-bond pathway for compound **4**, which is consistent with experimental data. Compound **5** is thermolyzed at a lower temperature than **4** (T_{avg} is 188 versus 240 °C), and the measured activation enthalpies are $\Delta H_1^\ddagger = 40.5 \pm 0.3$ and 45.9 ± 2.0 kcal/mol for **5** and **4**, respectively.

The endo-cyclopropane compounds differ from the remaining DBO compounds for two reasons: (1) the one-bond cleavage pathway is preferred over the two-bond cleavage pathway by 2–4 kcal/mol, and (2) both UB3LYP and CASPT2 methods predict that the diazenyl diradical intermediate will lose N_2 without a barrier, making TS(C-I) the rate-limiting step.

Cyclobutane-Fused Derivatives. The energetics of the decomposition of exo-fused-cyclobutane DBO, **6**, are listed in Table 1 and illustrated in Figure 9. The pathways for two-bond cleavage and one-bond cleavage converge at the formation of a twist-boat 1,4-diyl. Two-bond cleavage, **6-TS(B)**, has an activation enthalpy of 34.2 kcal/mol and forms this 1,4-diyl in a single concerted step. Alternatively, sequential one-bond cleavage, **6-TS(C-I)**, leads to the formation of a diazenyl diradical which then loses N_2 via **6-TS(C-II)** to form the 1,4-diyl. The rate-limiting step of this pathway is **6-TS(C-II)**, which has a relative enthalpy at 0 K of 37.4 kcal/mol and is ~ 3 kcal/mol higher in enthalpy than the two-bond cleavage pathway (B).

For the other DBO compounds predicted to decompose by diradical pathways (**2**, **4**, **5**, and **7**), the pericyclic three-bond

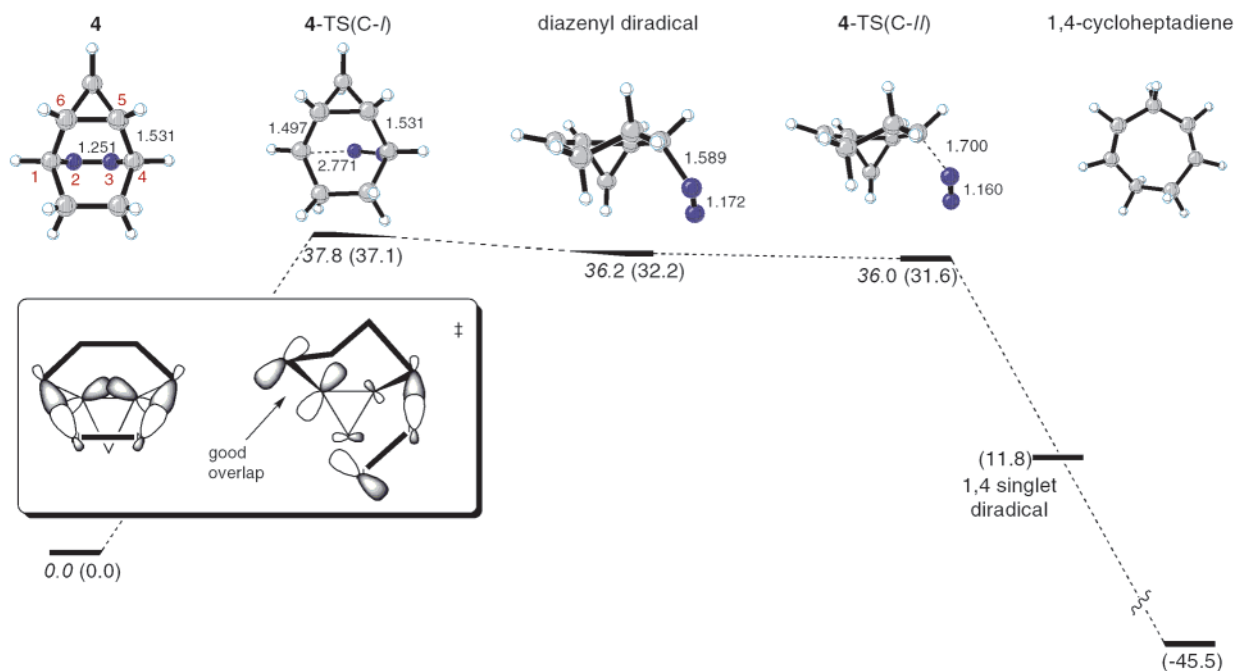


Figure 7. Deazetization of compound **4** by mechanism C. The bent bonds of the cyclopropane are orthogonal to the C–N bonds in the reactant. One-bond cleavage results in a typical cyclopropylcarbinyl geometry of the diazenyl intermediate. ΔH_{0K}^\ddagger values are in kcal/mol and correspond to (10,10)CASPT2 single points and (R and UB3LYP/6-31G* optimizations). Bond lengths are in Å.

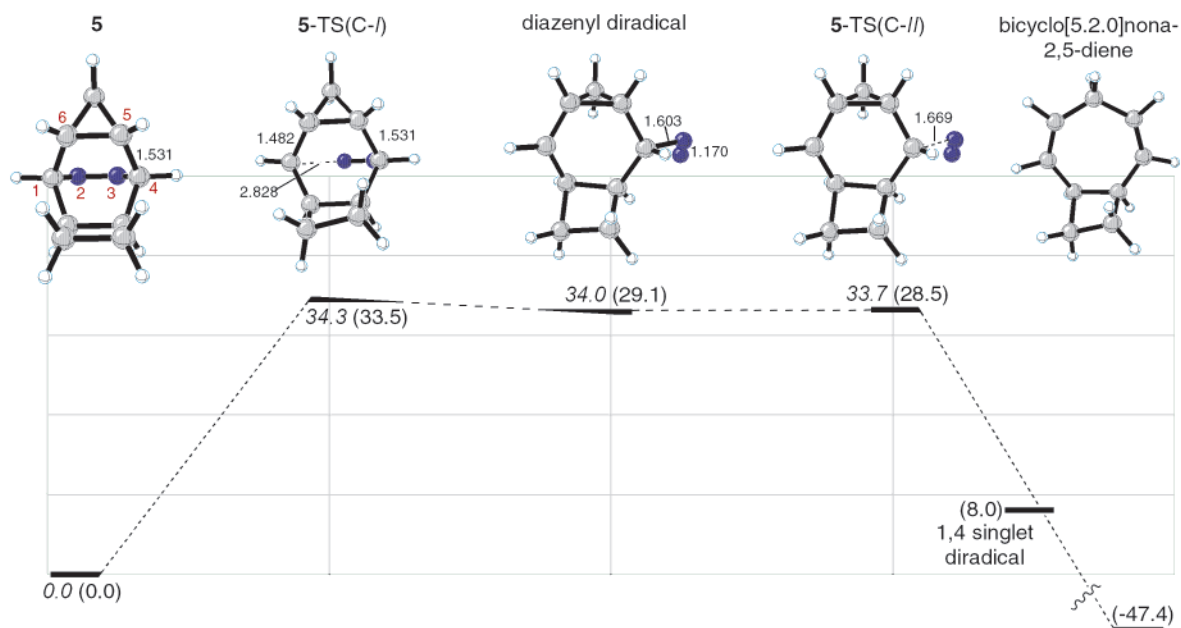


Figure 8. Deazetization of compound **5** by mechanism C. One-bond cleavage results in a typical cyclopropylcarbinyl geometry. ΔH_{0K}^\ddagger values are in kcal/mol and correspond to (12,12)CASPT2 single points and (R and UB3LYP/6-31G* optimizations). Bond lengths are in Å.

cleavage is sufficiently high in energy to predict that it will play no role in the decomposition of the DBO compound. Compound **6**, however, is an exception to this general trend. The pericyclic three-bond cleavage, **6-TS(A)**, has a barrier of 38.0 kcal/mol which is only 3–4 kcal/mol higher in enthalpy than the two-bond diradical pathway (B). Because the cyclobutane bond of **6** has less bent-bond character than a cyclopropane, the cyclic orbital overlap necessary for a facile [2+2+2] cycloreversion is much poorer than that in the analogous exocyclopropane compound, **3**.

Some involvement of **6-TS(A)** in the decomposition of **6** is supported by the observed experimental product distribution

found for decomposition of **6**. Both photolysis and thermolysis result in the loss of N_2 and lead to the formation of four major products: *cis,cis*-1,5-cyclooctadiene, *cis,trans*-1,5-cyclooctadiene, *trans*-tricyclo[4.2.0.0²⁻⁵]octane, and *cis*-divinylcyclobutane. As shown in Table 3, the product ratio is highly dependent on experimental conditions. Thermolysis of **6** at low pressure leads to a product mixture composed of 88% *cis,cis*-cyclooctadiene, the product which would be formed by concerted [2+2+2] cycloreversion. On the other hand, when **6** is photolyzed, or when tricyclooctane is thermolyzed, the decomposition pathway is required to proceed through a diradical, and the percent of *cis,cis*-cyclooctadiene is significantly lower. Our calculations

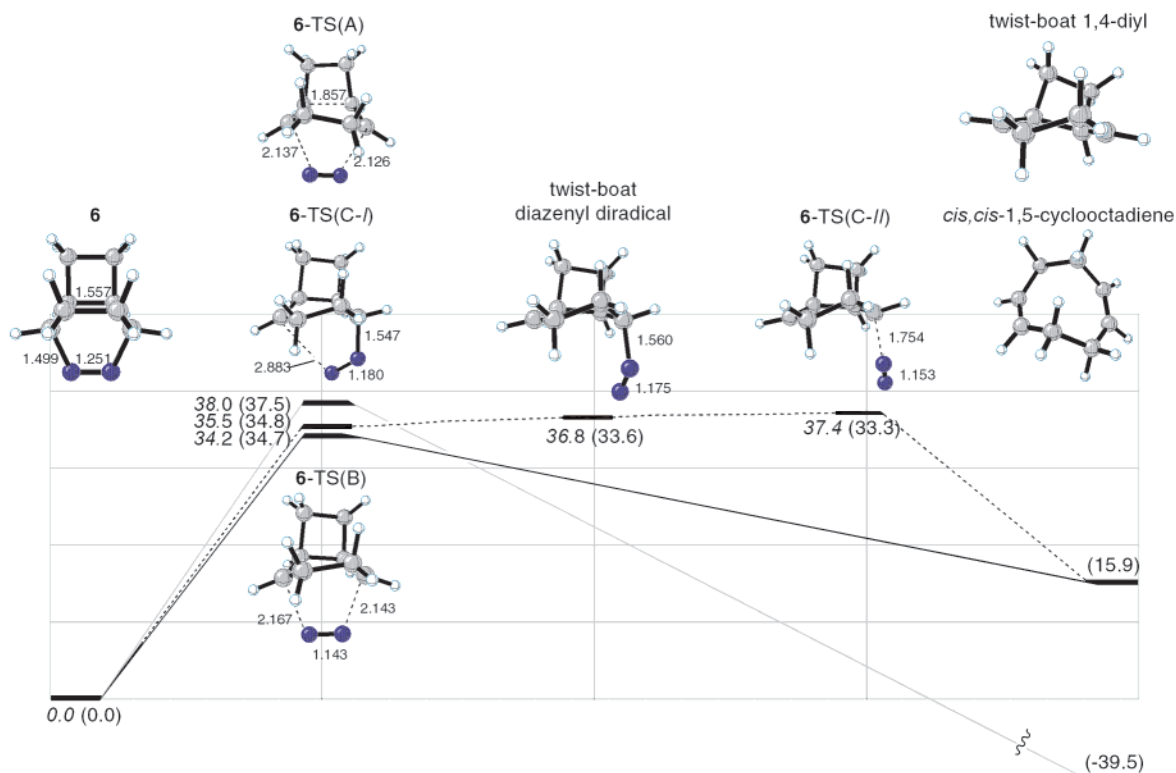
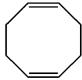
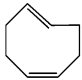
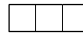
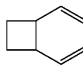


Figure 9. Deazetization of compound **6** by mechanisms A–C. ΔH_{0K}^\ddagger values are in kcal/mol and correspond to (12,12)CASPT2 single points and (R and UB3LYP/6-31G* optimizations). Bond lengths are in Å.

Table 3. Product Mixture from Thermolysis and Gas-Phase Photolysis of **6** and Cyclooctatriene¹⁷

Reactant	Conditions	Product mixture (%)			
					
6	290°C/ 34 torr	88	5	3	2
6	hν, pentane	13	53	22	12
6	hν, acetone	11	56	17	14
Tricyclooctane	290°C/34 torr	63	20	9	4
Tricyclooctane	300°C/14 torr	15	17	63	4

predict that pericyclic **6-TS(A)** is close in energy to the diradical pathways and corroborate the conclusion that decomposition of **6** lies on the border between a pericyclic and diradical regime.¹⁷

Compound **7**, the endo-fused-cyclobutane DBO, has not been examined experimentally, but computational results indicate that one-bond cleavage and two-bond cleavage are essentially isoenergetic (Figure 10, $\Delta H_{0K}^\ddagger = 41.4$ versus 41.7 kcal/mol). Simultaneous homolysis of both C–N bonds, **7-TS(B)**, leads to single-step formation of a twist-boat 1,4-diyl, the same intermediate formed by diradical loss of N₂ from compound **6**. However, unlike compound **6**, the one-bond cleavage transition structure, **7-TS(C-I)**, leads to the formation of a chairlike diazenyl diradical, which then loses N₂ in a subsequent step. The resulting chairlike 1,4-diyl is not a local minimum on the energy surface and collapses without a barrier to *cis,trans*-

1,4-cyclooctadiene. Under experimental conditions for thermolysis, the *cis,trans*-cyclooctadiene would be expected to undergo further rearrangement to the *cis,cis* isomer and also to tricyclooctane and divinylcyclobutane. The one-bond pathway for compound **7** most closely resembles the chairlike one-bond pathway for parent DBO compound **2**.

One point that needs to be further addressed is why isomer **6** undergoes one-bond cleavage to form a twist-boat 1,4-diyl whereas **7** undergoes one-bond cleavage to form a chairlike diyl. The transition structures **6-TS(C-I)** and **7-TS(C-I)** and their imaginary frequencies are shown in Figure 11. A comparison of the two structures reveals that both involve cleavage of the C1–N2 bond, accompanied by downward rotation of C8. The main difference is that **7-TS(C-I)** involves an additional downward rotation of C6 which is responsible for the boat-to-chair flip that occurs along with C–N bond cleavage.

One factor that may contribute to the different outcomes of one-bond cleavage is the degree of radical stabilization afforded

(17) Martin, H.-D.; Heiser, B.; Kunze, M. *Angew. Chem., Int. Ed. Engl.* **1978**, *17*, 696–697.

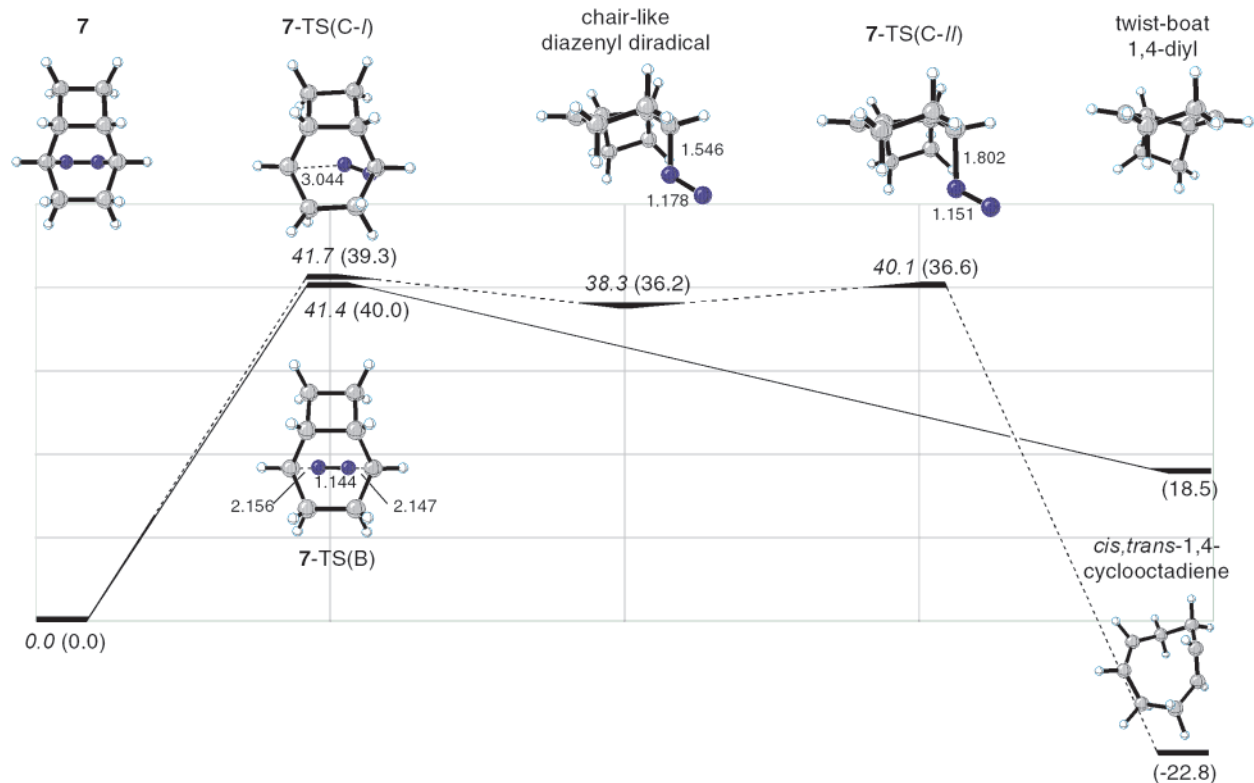


Figure 10. Deazetization of compound **7** by mechanisms B and C. ΔH_{0K}^\ddagger values are in kcal/mol and correspond to (12,12)CASPT2 single points and (R and UB3LYP/6-31G* optimizations). Bond lengths are in Å.

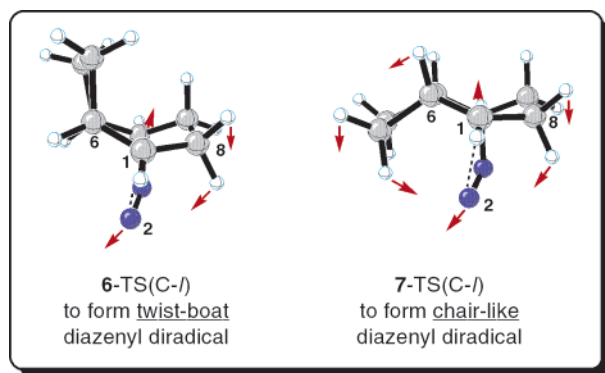


Figure 11. Imaginary frequency vectors for one-bond cleavage transition structures **6-TS(C-I)** and **7-TS(C-I)**.

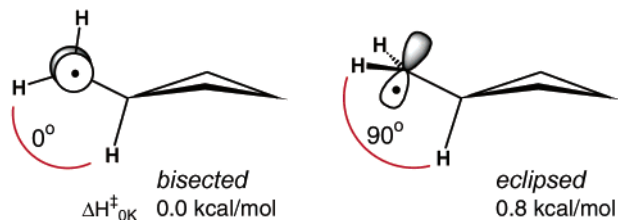


Figure 12. Two conformations of the cyclobutylcarbonyl radical. The bisected conformation is the global minima. The eclipsed conformer is a transition state for rotation of the $\bullet\text{CH}_2$ group.

by the fused cyclobutane ring. In the cyclobutylcarbonyl radical itself, UB3LYP/6-31G* predicts the bisected conformation to be ~ 0.8 kcal/mol more stable than the eclipsed conformation (Figure 12).

By analogy, the one-bond cleavage of **6** into a twist-boat geometry maintains a bisected orientation (15°) between the C1 radical and the cyclobutane CC framework (Figure 13). For **7**,

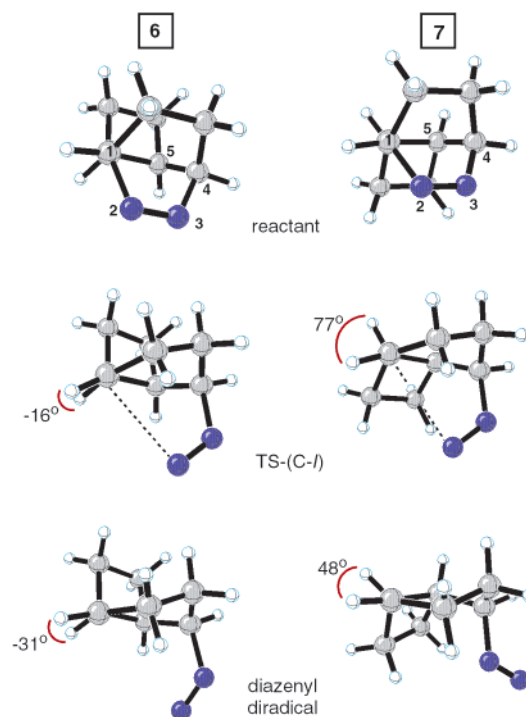
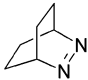
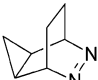
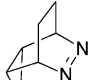
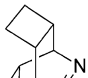
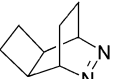
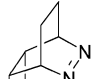


Figure 13. Newman projection along the C1–C6 bond for reactants **6** and **7**, the respective one-bond cleavage transition structures, and the resulting diazenyl diradical intermediates. Angles correspond to the HC1C6H dihedral.

one-bond cleavage into a chair increases the overlap between the C1 radical and the cyclobutane ring such that in **7-TS(C-I)**, the key dihedral angle is 77° , and in the chairlike diazenyl diradical, the dihedral angle has decreased to 48° . In contrast, the twist-boat diazenyl diradical produced from **7** has a dihedral

Table 4. Summary of the Experimental and Computational Activation Parameters for the DBO Series^a

Azoalkane	Experimental			Calculated			
	ΔH^\ddagger (kcal/mol)	ΔS^\ddagger (e.u.)	Average Temp (K)	Preferred Mechanism	$\Delta H^\ddagger_{\text{avgT}}$ (kcal/mol)	$\Delta S^\ddagger_{\text{avgT}}$ (e.u.)	$\Delta G^\ddagger_{\text{avgT}}$ (kcal/mol)
	43.6 ± 0.2	10.5 ± 0.3	509	TS(B)	42.8	11.1	37.1
	45.0 ± 0.2	10.6 ± 0.4		TS(C-Ia)	41.7	7.8	37.7
				diazenyl dirad	43.9	17.0	35.3
				TS(C-IIa)	44.3	16.1	36.1
				TS(C-Ib)	42.6	10.5	37.2
				TS(C-IIb)	39.6	13.0	33.0
	14.3 ± 1.5	-21	288	TS(A)	21.5	4.1	20.4
	21.5 ± 0.4	4.1 ± 1.1					
	45.9 ± 2.0	10.4 ± 3.8	513	TS(C-I)	38.8	5.2	36.1
				diazenyl dirad	38.6	13.9	31.5
				TS(C-II)	38.1	13.0	31.4
	40.5 ± 0.3	10.3	461	TS(B)	37.7	9.5	33.3
				TS(C-I)	35.4	6.4	32.5
				diazenyl dirad	36.4	15.5	29.3
				TS(C-II)	35.7	13.3	29.6
	38.3 ± 0.3	11	436	TS(B)	35.6	6.7	32.7
				TS(C-I)	36.6	4.3	34.7
				diazenyl dirad	38.8	11.7	33.7
				TS(C-II)	39.2	11.9	34.1
	N.A.	N.A.	509	TS(B)	43.2	11.8	37.2
				TS(C-I)	42.8	6.2	39.7
				diazenyl dirad	40.3	11.2	34.6
				TS(C-II)	42.0	12.9	35.5

^a Calculated values are CASPT2//UB3LYP energies with UB3LYP entropies, enthalpy corrections, and free energy corrections.

angle of 83°; thus, no increase in radical stabilization would be gained. All attempts to locate transition structures leading to the chairlike diazenyl diradical from **6** or a twist-boat diazenyl diradical from **7** have failed.

Summary of Decomposition Mechanisms for Diazabicyclo[2.2.2]octenes. Table 4 summarizes the experimental activation parameters and the calculated enthalpy, entropy, and free energy of activation at the average experimental temperature for each DBO compound. Only the competitive mechanisms are listed. Several conclusions can be drawn from Table 4.

(1) In general, the calculated $\Delta H_{\text{avgT}}^\ddagger$ value agrees well with the corresponding experimental value, although the calculated diradical barriers tend to be 1–3 kcal/mol lower than the experimental barriers. The exception to this trend is compound **4**, where the $\Delta H_{\text{avgT}}^\ddagger$ value is ~7 kcal/mol lower than the $\Delta H_{\text{exp}}^\ddagger$ value. For the thermolysis of **3**, the calculated parameters for three-bond cleavage ($\Delta H_{288\text{K}}^\ddagger = 21.5$ kcal/mol and $\Delta S_{288\text{K}}^\ddagger = 4.1$ eu) are in better agreement with the kinetic data reported by Snyder and Harpp for isoctane solvent ($\Delta H^\ddagger = 21.5$ kcal/mol, $\Delta S^\ddagger = 4.1 \pm 1.1$ eu)^{5d} than with the kinetic data reported by Allred and Hinshaw for liquid pyridine-cuprous chloride.

(2) For the twist-boat one-bond mechanism, TS(C-I) generally has a lower enthalpy and entropy than TS(C-II). At higher temperatures, the role of entropy becomes increasingly important, and the free energy of TS(C-I) may become higher than that of TS(C-II). Such a reversal is observed for compounds **2**, **5**, and **6**. For the chairlike one-bond mechanism, no temperature-

dependent reversal is observed because the first step, TS(C-I), has a higher enthalpy and lower entropy than TS(C-II).

(3) Only two compounds in the DBO series have a strong preference for a single mode of decomposition: **3** decomposes by a concerted three-bond cleavage (mechanism A), and **4** decomposes by a one-bond cleavage (mechanism C). The remaining compounds, **2**, **5**–**7**, all have one-bond and two-bond diradical pathways that are expected to be competitive at the average temperature for thermolysis.

The CASPT2[g₃] method¹⁸ has been applied to several of the DBO stationary points, including the parent, **2**. This method uses a new one-particle zeroth-order Hamiltonian designed to give a more balanced description of CASSCF reference wave functions that are dominated by both closed-shell and open-shell configurations. The new partitioning can lead to better excitation energies and dissociation energies. For the azoalkane systems, the energy gap between the one-bond and two-bond pathways is affected very little; the preference for two-bond increases by ~0.3 kcal/mol. However, when CASPT2[g₃] is used instead of CASPT2, the relative enthalpies of the diradical intermediates and transition structures increase by 0.5–1.6 kcal/mol. Consequently, the CASPT2[g₃] values show slightly better agreement with the experimental activation enthalpies because the CASPT2 values tended to be lower than the experimental values (Table 4).

(18) Andersson, K. *Theor. Chim. Acta* **1995**, *91*, 31–46.

Table 5. Stationary Points Involved in the Thermolysis of *trans*-Azomethane, As Calculated at Various Levels of Theory^a

methodology	TS(B)	Me-N=N [•] + Me [•]	TS(C- <i>I</i>) cleave Me-N=N [•] + Me [•]		N ₂ + 2Me [•]	reaction coordinate type (Figure 14)
(U)B3LYP/6-31G(d)	*	48.6 ^{14b}	51.4	(2.8)	34.5	1
(U)B3LYP/6-311G(d,p)	50.0	46.3	47.9	(1.6)	28.4	1
(6,6)CASPT2/6-31G(d)//UB3LYP/6-311G(d,p)	50.2	47.8	51.9	(4.1)	28.0	3
(10,8)CASPT2/6-31G(d)//UB3LYP/6-311G(d,p)	49.3	46.8	50.1	(3.3)	26.9	3
(4,4)CASPT2/6-31G(d)//(4,4)CASSCF/6-31G(d) ¹⁰	46.6	43.3	46.2	(2.9)	23.3	1
(6,6)CASPT2/6-31G(d)//(6,6)CASSCF/6-31G(d)	48.0	46.6	47.5	(0.9)	24.8	1
(10,8)CASPT2/6-31G(d)//(10,8)CASSCF/6-31G(d)	47.0	45.3	46.7	(1.4)	23.6	1
MP2/6-311G(2d,p) ^{14a}	60.5	58.3	61.2	(2.9)	22.8	3
MP4SDQ/6-311G(2d,p)//MP2/6-311G(2d,p) ^{14a}	63.3	50.9	52.5	(1.6)	18.4	1
QCISD(T)/6-311G(2d,p)//MP2/6-311G(2d,p) ^{14a}	44.2	51.5	51.8	(0.3)	22.2	2
CCSD(T)/cc-pVTZ//MP2/6-311G(2d,p) ^{14a}	45.2	52.0	52.2	(0.2)	21.0	2
CCSD(T)/TZ2P//CISD/TZ2P ^{14c,d}	*	46.3	48.6	(2.3)	~24.8	1
G3(MP2)/6-31G(d) ^{14b}	45.4	54.0				
QCISD/6-311G(d,p) ^{14c}				(~1.0)		

^a All energies (ΔH_{0K}) are reported in kcal/mol relative to *trans*-azomethane and include ZPE correction. Energies in parentheses indicate the barrier height for the C–N cleavage in methyl-diazenyl radical. All reported energies include the zero-point energy correction. ZPE corrections in ref 14a were estimated from MP2/6-311G(2d,p) frequencies scaled by 0.93. ZPE correction in ref 14c was estimated from QCISD/6-31G(d). The * indicates that the location of such a structure was attempted but not successful.

The DBO derivatives exhibit a range of mechanisms subtly tuned and controlled by additional small ring fusions. It is of interest to compare these results to those obtained for simpler and more extensively studied systems, **AM** and **DBH**.

Azomethane. Numerous calculations and experimental studies have been conducted on the decomposition of azomethane, the simplest of acyclic azoalkanes.^{7,14} Table 1 lists the experimentally determined activation energies for the thermolysis of *trans*-azomethane. The reported values, which were previously summarized by Engel,^{1a} come from several different laboratories⁷ and range from 50.2 to 55.4 kcal/mol. The average E_a is 52.1 kcal/mol.

The energies of intermediates and transition structures potentially involved in the decomposition of *trans*-azomethane are summarized in Table 5 and Figure 14. Computational methods are inconclusive about whether there is a transition structure corresponding to concerted two-bond cleavage. Of the seven methods used to search for a concerted two-bond cleavage, TS(B), such a transition structure was found with five methods but not with two of the methods. A correct description of the two-bond cleavage appears to be sensitive to the size of the basis set.^{14a,c} This is apparent in the absence of a two-bond cleavage transition structure with UB3LYP/6-31G(d), whereas the transition structure was located with UB3LYP/6-311G(d,p). The G3 method involves optimization at the UHF/6-31G(d) level, and no TS was found; however, when the full MP2 method was included in the structure optimization (known as G3(MP2)), the concerted transition structure was located.^{14b} The computed barrier for two-bond cleavage ranges from 44.2 to 63.3 kcal/mol. A majority of the methods predict TS(B) to be between 44 and 50 kcal/mol, while perturbation theory (MP2) predicts TS(B) to be >60 kcal/mol.

A transition structure for one-bond cleavage, TS(C-*I*), has not been located at any level of theory, indicating that the methyl-diazenyl and methyl radicals recombine with no enthalpic barrier. The methyl radical/diazenyl radical pair lies approximately 50 kcal/mol higher in energy than *trans*-azomethane. TS(C-*II*), the transition structure for cleavage of the C–N bond of the diazenyl radical, ranges from 0.2 to 4.1 kcal/mol higher

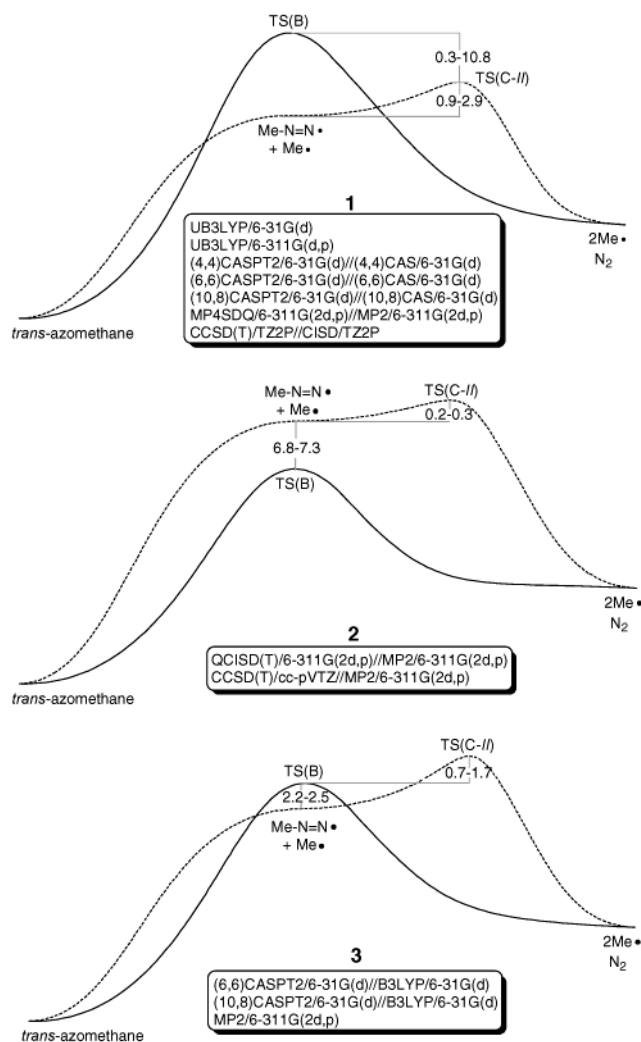


Figure 14. Three patterns of reaction coordinates obtained for the competing one-bond and two-bond mechanisms for thermal decomposition of *trans*-azomethane. ΔH_{0K}^\ddagger values are given in kcal/mol.

in energy than the methyl-diazenyl intermediate. These calculations indicate that the methyl-diazenyl radical is a bound species

Table 6. A Comparison of Optimized Geometries Obtained by Various Computational Methods for Important Stationary Points in the Decomposition of *trans*-Azomethane^a

	<i>trans</i> -azomethane			TS(B)			methyl diazenyl			TS(C-II)		
	CN	NN	<CNN	CN	NN	<CNN	CN	NN	<CNN	CN	NN	<CNN
(U)B3LYP/6-31G(d)	1.478	1.242	112				1.509	1.179	122	1.856	1.141	119
(U)B3LYP/6-311G(d,p)	1.465	1.236	113	2.126	1.133	112	1.513	1.170	123	1.821	1.135	120
(4,4)CAS/6-31G(d) ¹⁰	1.487	1.211	113	2.076	1.130	109	1.528	1.161	118	1.749	1.135	115
(6,6)CAS/6-31G(d)	1.495	1.235	112	2.047	1.149	109	1.590	1.171	117	1.654	1.162	116
(10,8)CAS/6-31G(d)	1.499	1.233	112	2.039	1.148	109	1.574	1.168	120	1.678	1.155	119
MP2/6-311G(2d,p) ^{14a}	1.464	1.253	112	2.226	1.127		1.507	1.141	126	1.777	1.114	122
CISD/TZ2P ^{14c,14d}	1.458	1.220	113				1.485	1.161	122	1.779	1.121	119
QCISD/6-31G(d) ^{14e}							1.508	1.192	121	1.809	1.156	118
Experimental ¹⁹	1.474	1.254	111.9									
	±0.003	±0.003	±0.5									
	1.482	1.247	112.3									
	±0.002	±0.003	±0.3									

^a Bond lengths are given in Å, and bond angles are given in degrees.

but should exhibit a very short lifetime before decomposing into N₂ and a methyl radical.

As shown in Figure 14, the reaction coordinate patterns calculated for *trans*-azomethane can be divided into three categories based on the relative energies of TS(B), TS(C-II), and the radical intermediates. In category 1, the barrier for two-bond cleavage is predicted to be higher in energy than the one-bond cleavage pathway. In category 2, the barrier for two-bond cleavage is predicted to be lower in energy than the one-bond cleavage pathway. In category 3, the barrier for two-bond cleavage is intermediate, and it falls between the energies of the radical intermediates and the TS(C-II) of the one-bond pathway. As would be expected, this type of reaction coordinate is more likely to occur when the barrier for C–N cleavage of the methyl-diazenyl radical is relatively large (>2 kcal/mol).

CASSCF and UB3LYP optimized geometries show significant differences in C–N and N=N bond lengths (Table 6). For example, (6,6)CASSCF/6-31G(d) predicts that the C–N bond is stretched 0.552 Å in going from *trans*-azomethane to TS(B) and 0.063 Å in going from methyl-diazenyl radical to TS(C-II). In contrast, UB3LYP/6-311G(d,p) predicts these changes in C–N to be 0.697 and 0.308 Å, respectively.

The differences in the CASSCF¹⁰ and UB3LYP optimized geometries are due to the differing shapes of the reaction coordinate for the conversion of the methyl-diazenyl radical to the N₂/methyl radical pair. Scans of the C–N bond distance, shown in Figure 15, indicated that although UB3LYP, (4,4)-CASSCF, and (6,6)CASSCF all predict a barrier to cleavage of the C–N bond, the position of the transition structure varies significantly among the methods (Figure 15, filled points). On the other hand, the CASPT2 single points (Figure 15, open points) show excellent agreement in both the height and the position of the transition structure regardless of the optimization method. Similar results were reported by Adam, Olivucci, et al. using a (12,10) active space. They showed that the reaction coordinates generated with CASPT2//CASSCF, CASPT2 optimization (using numerical gradients) and DFT were in good agreement with each other but differed significantly with the

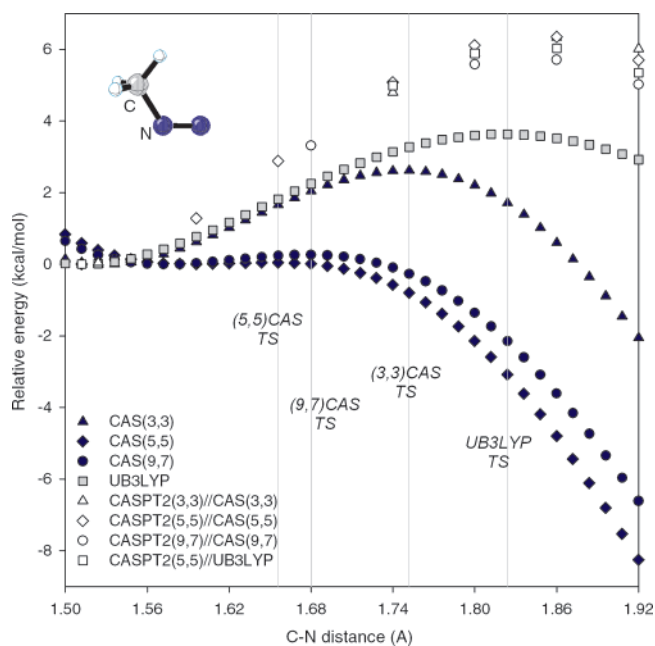
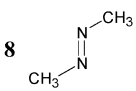


Figure 15. Change in the relative energy (ZPE exclusive) of the methyl-diazenyl radical as the C–N bond distance is increased from 1.50 to 1.92 Å.

(12,10)CASSCF surface.¹⁶ In accord with the results for the DBO parent system, UB3LYP is superior to CASSCF for locating appropriate geometries for the cleavage of diazenyl radical (or diradical) systems.

In predicting whether the one-bond or two-bond mechanism is operative for AM at the experimental temperature, the free energy surfaces must be analyzed because the inclusion of entropy significantly alters the shape of the one-bond pathway. A barrier for recombination of methyl-diazenyl radical plus methyl radical exists on the one-bond free energy surface because the entropy decreases when the two radical species are brought together in the proper orientation. In such a case, a maximum on the free energy surface, corresponding to TS(C-I), can be located using the variational transition state

Table 7. Summary of the Experimental and Computational Activation Parameters for AM, **8**^a

Azoalkane	Experimental			Mechanism	Calculated		
	ΔH^\ddagger (kcal/mol)	ΔS^\ddagger (e.u.)	Average Temp (K)		ΔH^\ddagger_{565K} (kcal/mol)	ΔS^\ddagger_{565K} (e.u.)	ΔG^\ddagger_{565K} (kcal/mol)
	50.1 ± 0.3	10.1 ± 0.7	565	TS(B)	53.3	22.4	40.7
	54.4 ± 0.6	17.5 ± 1.0		TS(C-I)	47.2	13.4	39.6
	51.3	14.1		Me-N=N• + Me•	50.1	43.3	25.6
	51.3	13.6		TS(C-II) + Me•	54.3	45.5	28.5
	49.1	10.9					

^a Calculated values are (6,6)CASPT2/6-31G**//UB3LYP/6-311G** energies with UB3LYP entropies, enthalpy corrections, and free energy corrections.

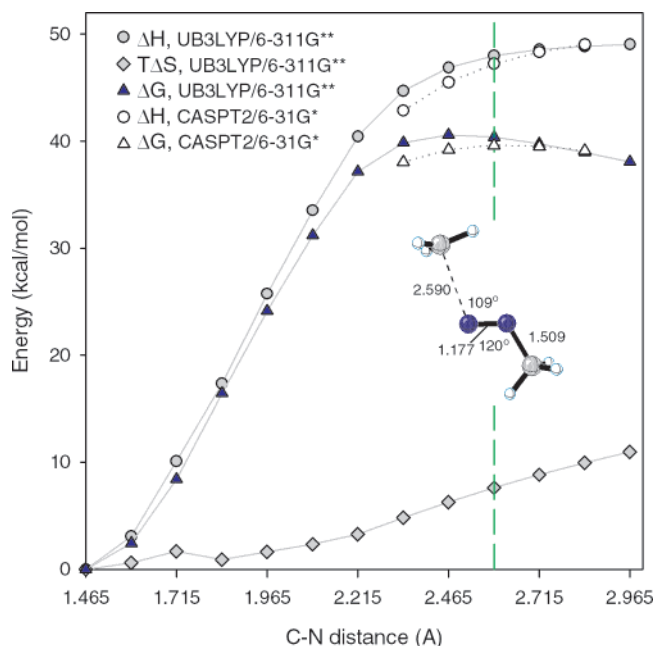


Figure 16. Change in the relative enthalpy, free energy, and $T\Delta S$ of *trans*-azomethane as one C–N bond distance is increased from 1.564 to 2.965 Å. A transition state on the ΔG surface is located when the C–N bond distances are 1.509 and 2.590 Å.

theory.²⁰ The position of TS(C-I) was approximated by using UB3LYP/6-311G(d,p) to scan one C–N bond length of **AM** from 1.465 to 3.215 Å; the remaining degrees of freedom were fully optimized (Figure 16). Vibrational analysis at each point was used to compute the entropies and free energies at 565 K. The approximate TS(C-I) occurs when one C–N is stretched to 2.590 Å and the second C–N bond is 1.509 Å.

Table 7 and Figure 17 summarize the calculated activation parameters for *trans*-azomethane at the average experimental temperature, 565 K. For the one-bond pathway, cleavage of the first C–N bond is now the rate-limiting step ($\Delta G_{565K}^\ddagger = 39.6$ kcal/mol) but is only slightly lower than the rate-limiting step of the two-bond pathway (40.7 kcal/mol) which translates to a ~2.7:1 preference for the one-bond pathway. Assuming that these results are similar to the DBO results in that the $\Delta H_{\text{avgT}}^\ddagger$ values may be underestimated by 1–3 kcal/mol, we determined that the one-bond activation parameters show better agreement with the experimental values.

2,3-Diazabicyclo[2.2.1]hept-2-ene. Many quantum mechanical and molecular dynamics studies have been conducted on

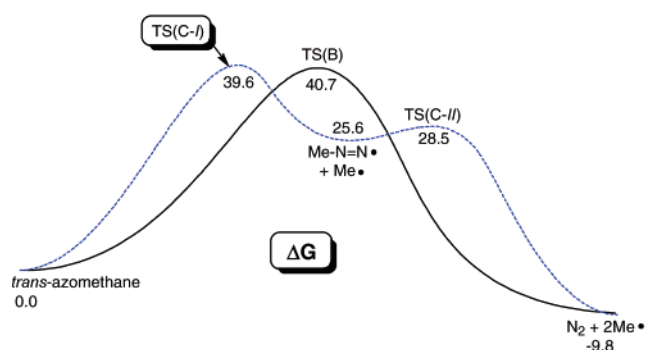
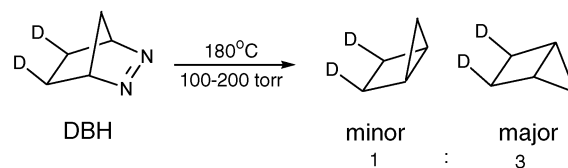


Figure 17. The free energy reaction coordinate for competing one-bond and two-bond decomposition of *trans*-azomethane. Free energies are given in kcal/mol.

the decomposition of the diazabicycloheptene, **DBH**. The primary focus has been on explaining the experimental observation by Roth and Martin in 1967 that *exo,exo*-5,6-*d*₂-**DBH** preferentially forms the inverted bicyclopentane product.²¹



Reyes and Carpenter² have thoroughly discussed the various hypotheses explaining the formation of the inverted product,^{21,22} the experimental background relevant to the question of one-bond versus two-bond cleavage,²³ the role of dynamics,^{24,25} and the use of multiconfigurational computational methods;²⁶ consequently, these topics will not be discussed here. Here, the numerous quantum mechanical calculations that have been performed on the potential surface of **DBH** are summarized and compared.

The experimental activation enthalpy for thermolysis of **DBH** has been measured as 36.5 ± 0.3 and 36.0 ± 0.2 kcal/mol (Table 1).⁸ The calculated barriers for the two-bond versus one-bond diradical mechanisms are shown in Table 8. The calculated

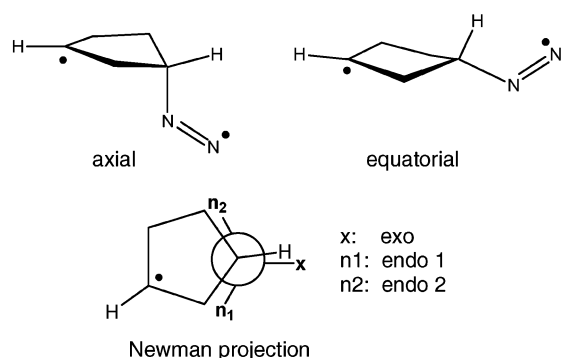
- (19) Electron diffraction studies: (a) Chang, C.-H.; Porter, R. F.; Bauer, S. H. *J. Am. Chem. Soc.* **1970**, *92*, 5313–5318. (b) Almennigen, A.; Anfinsen, I. M.; Haaland, A. *Acta Chem. Scand.* **1970**, *24*, 1230–1234.
 (20) Cramer, C. J. *Essentials of Computational Chemistry, Theories and Models*; John Wiley & Sons, Ltd: West Sussex, England, 2002; pp 483–485.

- (21) (a) Roth, W. R.; Martin, M. *Justus Liebigs Ann. Chem.* **1967**, *702*, 1–7. (b) Roth, W. R.; Martin, M. *Tetrahedron Lett.* **1967**, 4695–4698.
 (22) Allred, E. L.; Smith, R. L. *J. Am. Chem. Soc.* **1967**, *89*, 7133–7134.
 (23) Simpson, C. J. S. M.; Wilson, G. J.; Adam, W. *J. Am. Chem. Soc.* **1991**, *113*, 4728–4732.
 (24) Lyons, B. A.; Pfeifer, J.; Peterson, T. H.; Carpenter, B. K. *J. Am. Chem. Soc.* **1993**, *115*, 2427–2437.
 (25) Sorescu, D. C.; Thompson, D. L.; Raff, L. M. *J. Chem. Phys.* **1995**, *20*, 7910–7924.
 (26) (a) Yamamoto, N.; Olivucci, M.; Celani, P.; Bernardi, F.; Robb, M. A. *J. Am. Chem. Soc.* **1998**, *120*, 2391–2407. The (6,5) active space included one set of C–N σ/σ^* orbitals, the N=N π/π^* orbitals, and one lone pair orbital.

Table 8. Stationary Points Involved in the Thermolysis of DBH, As Calculated at Various Levels of Theory^a

methodology	TS(B)	cyclopentyl-diazenyl diradical				barrier for TS	cyclopentane diyl + N ₂	rxn coord. type (Figure 18)
		conformer	minima	TS(C-I)				
(U)B3LYP/6-31G(d)	34.9	ax-exo	33.1	33.9	(0.7)	17.1	1	
		ax-endo1		33.4	(0.2)			
		ax-endo2	33.3	33.5	(1.8)			
		eq-exo	32.9	34.7	(1.1)			
		eq-endo1	33.1	34.2	(1.3)			
		eq-endo2	34.1	35.4				
(6,6)CASPT2/6-31G(d)//UB3LYP	35.0	ax-exo	37.0	39.8	(2.8)	2		
		eq-exo	37.4	40.0	(2.6)			
(4,4)CASPT2/6-31G(d)//(4,4)CASSCF ¹⁰	31.3	ax-exo	C ₂ 34.3	36.5	(2.2)	2		
		eq-exo	C _S 34.6	36.3	(1.7)			
(6,6)CASPT2/6-31G(d)//(6,6)CASSCF ^{2,c}	32.4	eq-endo1	C _S ~39.0		(~0.0)	22.7 (C ₂)	2	
(10,8)CASPT2/6-31G(d)//(10,8)CASSCF	31.8	ax-exo	C ₂ 36.8	37.3	(0.6)	2		
(12,10)CASPT2/6-31G(d)//(12,10)CASSCF ¹⁶	31.8	eq-exo ²	C _S		(1.1) ^b			
		ax-exo	C ₂		(2.7) ^b			
		ax-exo	C _S		(3.6) ^b			
		eq-exo	C _S		(2.2) ^b			
MP2//((6,5)CASSCF/6-31G(d)) ²⁶	29.8 ^{6,6}	ax-exo	C ₂ 24.8	29.9	(5.1)	3		
		ax-endo2	C _S 23.6					
		ax-ex/en2	C ₂ 29.8 ^b					
HF/6-31G(d) ^{25,d}	75.0				(~6.3)			

^a All energies (ΔH_{0K}) are reported in kcal/mol and include ZPE correction. Energies in parentheses indicate the barrier height for the C–N cleavage in the cyclopentyl-diazenyl radical. ^b ZPE correction not included. ^c Frequencies scaled by 0.892. ^d Frequencies scaled by 0.893.



ΔH_{0K}^\ddagger values for the concerted two-bond cleavage range from 29.8 to 35.1 kcal/mol, with the HF activation enthalpy being much higher, as expected. None of the computational methods were able to locate a one-bond cleavage TS(C-I) connecting the reactant and the cyclopentyl-diazenyl diradical. As found for **AM**, stretching a single C–N bond of the reactant gives rise to a Morse-like potential with no maximum on the potential energy surface for bond cleavage. Many conformations of the cyclopentyl-diazenyl diradical can be located due to the conformation flexibility of the five-membered ring (categorized here as having the diazenyl group either axial or equatorial) and the rotational freedom of the pendant diazenyl group (exo, endo1, and endo2). Most of the methods find that the cyclopentyl-diazenyl diradical is bound, and the barrier for loss of N₂ ranges from ~0 to 5.1 kcal/mol.

As shown in Table 8, UB3LYP predicts that the two-bond cleavage pathway is slightly higher in enthalpy than the one-bond cleavage pathway, corresponding to a type 1 reaction coordinate. The UB3LYP predictions for **DBH** match what was found for the DBO enthalpy surfaces: this method tends to overestimate the stability of both the diazenyl diradical and the subsequent one-bond cleavage transition structure, TS(C-II), making the one-bond pathway energetically favorable as compared to the two-bond pathway. The CASPT2//UB3LYP

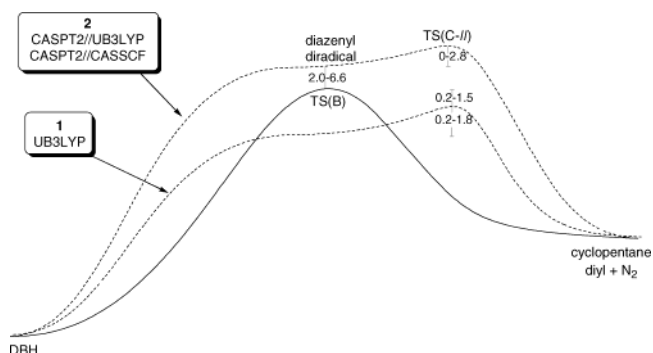


Figure 18. Two most common patterns of reaction coordinate predicted for the thermal decomposition of **DBH**. ΔH_{0K}^\ddagger values are given in kcal/mol. The two-bond cleavage (heavy line) is preferred over one-bond by CASPT2, but not UB3LYP.

method corrects the overestimated stability of the one-bond pathway and predicts that concerted synchronous two-bond cleavage is favored by ~5 kcal/mol relative to the one-bond surface (type 2 surface). CASPT2//CASSCF with (4,4), (6,6), and (10,8) active spaces also predicts a type 2 surface. When CASPT2//CASSCF methodology is used, the two-bond cleavage is favored over the one-bond cleavage by more than 5 kcal/mol. These results are summarized in Figure 18.

The shapes of the one-bond reaction coordinate corresponding to the loss of N₂ from the diazenyl diradical are highly dependent on the computational method used for optimization (Figure 19). On one extreme are (6,6)CASSCF and (10,8)CASSCF results, which predict that the cyclopentyl-diazenyl diradical is unbound or only slightly bound. On the other extreme are (4,4)CASSCF and UB3LYP, which predict more substantial barriers for loss of N₂ from the cyclopentyl-diazenyl diradical. The CASPT2 single point energies confirm that there is indeed a barrier for cleavage of the C–N bond of the diazenyl diradical and that the position of the transition structure is relatively late (C–N distance ~1.86 Å). The differences in the calculated one-bond surfaces are also reflected in the geometric parameters of the

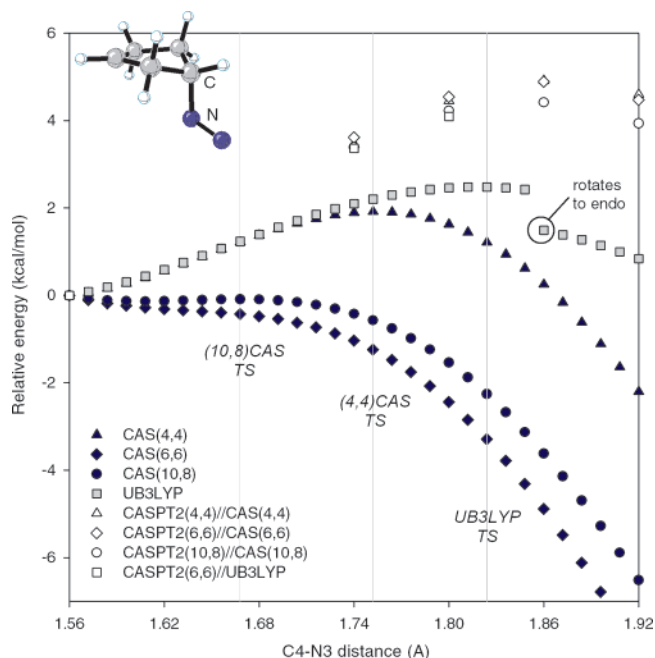


Figure 19. Change in the relative energy (ZPE exclusive) of the cyclopentyl-diazenyl diradical (conformation axial-exo) as the C–N bond distance is increased from 1.56 to 1.92 Å. Similar results are found for the cyclopentyl-diazenyl diradical in the equatorial-exo conformation.

optimized intermediates and transition structures shown in Figure 20. Similar observations were made by Adam, Olivucci, et al.¹⁶

The pyramidalization of the alkyl radical center of the **DBH** diazenyl diradical is another parameter that is highly dependent on the optimization method. UB3LYP geometry optimization predicts that the alkyl radical is approximately planar, that is, sp^2 hybridized. CASSCF optimization predicts that the alkyl radical is pyramidalized. Adam, Olivucci, et al. recently categorized the CAS optimized structures as either C_2 -like or

C_5 -like, referring to the approximate symmetry of the H1 and H5 atoms (Figure 21). The difference in the UB3LYP and CASSCF structures was investigated here by driving the H1C2C3H4 dihedral angle from 20° to 70° while allowing all other parameters to fully optimize. CASPT2 single point energies were also evaluated for each of the UB3LYP and (4,4)-CASSCF structures. With respect to the H1C2C3H4 dihedral angle, the radical at C2 is C_2 -like from 20° to 40°, approximately planar from 45° to 50°, and C_5 -like from 55° to 70°. As shown in Figure 21, UB3LYP predicts a minimum for the diazenyl diradical to occur at ~45°, such that the carbon-centered radical is planar. (6,6)CASPT2//UB3LYP predicts the potential energy well has a similar shape with the energy minimum located at ~38°, corresponding to a slight C_2 -like geometry. (4,4)CASSCF predicts that the H1C2C3H4 reaction coordinate has a dramatically different shape with a global minimum at 30° and a very shallow minimum (or inflection point) at 55° that is higher in energy by only 0.2 kcal/mol. Inclusion of correlation energy with the (4,4)CASPT2//(4,4)CAS method results in a surface more similar to the UB3LYP surface in that only one distinct minimum can be located at ~48°. On the basis of these results, we conclude that the C_2 -like and C_5 -like geometries for the DBH diazenyl diradical are not “distinct mechanistic entities” in contrast to the Adam, Olivucci, et al. conclusion.¹⁶ Nevertheless, both geometries are easily accessible because the reaction coordinate for pyramidalizing the secondary alkyl radical is very shallow. The abbreviations C_2 and C_5 have been included in Table 8.

The optimized transition structure TS(C-II) in the equatorial-exo conformation deserves further comment (Figure 17). In this transition structure, stretching of the C–N bond is accompanied by CC bond formation, analogous to the Roth and Martin mechanism proposed to account for inversion of the cyclopentyl skeleton.^{21b} More recently, such a transition structure has been proposed to account for the inversion observed in the photo-

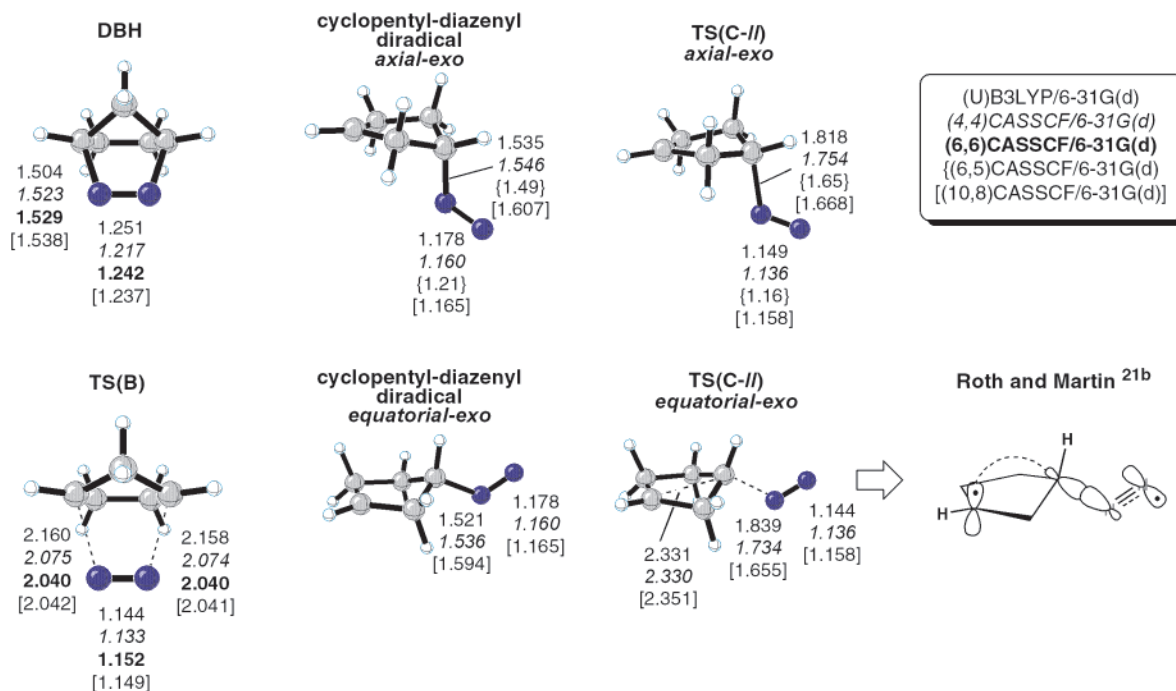
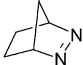


Figure 20. Selected **DBH** diradical transition structures and intermediates optimized using UB3LYP, (4,4)CASSCF,¹⁰ (6,6)CASSCF,² (6,5)CASSCF,^{26a} and (10,8)CASSCF. Bond lengths are given in Å.

Table 9. Summary of the Experimental and Computational Activation Parameters for **DBH**, **9**^a

Azoalkane	Experimental			Mechanism	Calculated		
	ΔH^\ddagger (kcal/mol)	ΔS^\ddagger (e.u.)	Average Temp (K)		ΔH^\ddagger_{445K} (kcal/mol)	ΔS^\ddagger_{445K} (e.u.)	ΔG^\ddagger_{445K} (kcal/mol)
9 	36.5 ± 0.3	8.7 ± 0.4	445	TS(B)	36.6	9.1	32.5
	36.0 ± 0.2	5.8 ± 0.5		diazenyl dirad ax	39.0	12.4	33.5
				diazenyl dirad ex	39.4	12.2	34.0
				TS(C-I) ax	41.8	14.9	35.2
				TS(C-I) ex	42.1	14.6	35.6

^a Calculated values are (6,6)CASPT2//UB3LYP energies with UB3LYP entropies, enthalpy corrections, and free energy corrections.

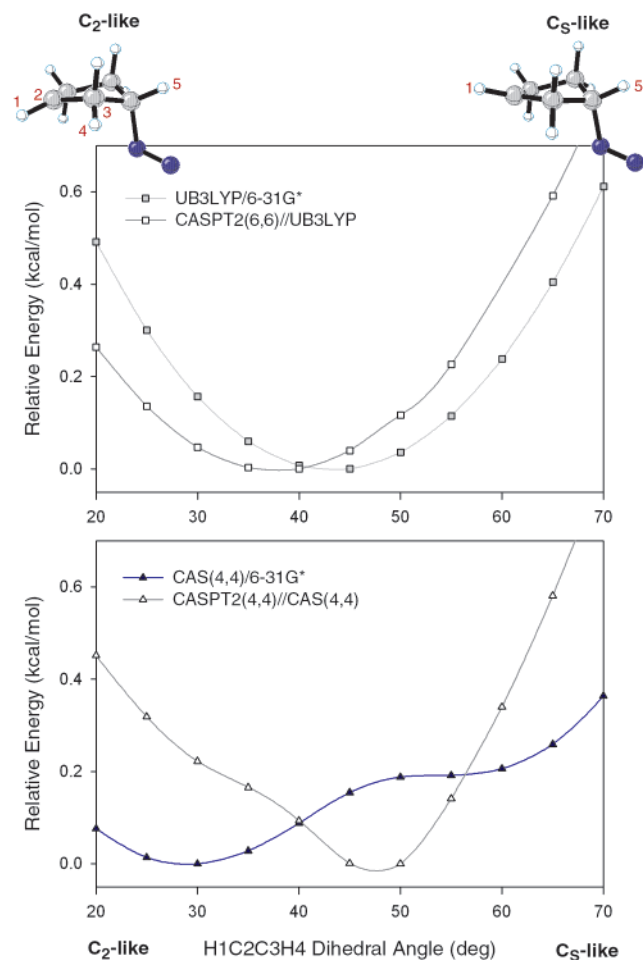


Figure 21. Change in the relative energy (ZPE exclusive) of the **DBH** cyclopentyl-diazenyl diradical (conformation axial-exo) as the H1C2C3H4 dihedral is rotated from 20° to 70°.

chemical deazetization of **DBH**.¹⁶ The relative free energy of this stationary point lies ~3 kcal/mol higher than that of the concerted diradical transition structure **TS(B)** (see Table 9); consequently, less than 5% of **DBH** would be expected to lose N₂ by a thermal one-bond pathway. This is consistent with the (6,6)CASPT2//((6,6)CASSCF) calculations by Reyes and Carpenter.²

Final Discussion of CASPT2, UB3LYP, and CASSCF. In the reactions studied here, CASPT2//UB3LYP and UB3LYP have shown excellent agreement in predicting the energies of diradical transition structures **TS(B)** and **TS(C-I)**. In general, the predicted relative energies of **TS(B)** or **TS(C-I)** differ by less than 1.0 kcal/mol, with **3-TS(C-I)** being the only exception. CASPT2//UB3LYP systematically calculates diazenyl diradicals

to be 3–4 kcal/mol higher in energy than predicted by UB3LYP. CASPT2//UB3LYP results for the parent and cyclobutane-fused systems indicate that the diazenyl diradical is a bound species requiring an additional 1–2 kcal/mol for cleavage of the second C–N bond, and this corresponds to the rate-limiting step for the one-bond twist-boat cleavage pathway. When an endo-fused cyclopropane is present in the system, **4** and **5**, the barrier for cleavage of the second C–N bond is absent, resulting in **TS(C-I)** becoming the rate-limiting step. In contrast, UB3LYP predicts that not only **4** and **5**, but all members of the **DBO** series have very small or nonexistent barriers for cleavage of the second C–N bond, **TS(C-I)**. Although UB3LYP predicts barriers that are too small, the shape of the potential energy surface for the conversion of the diazenyl diradical to N₂ plus diyl is similar to that of the CASPT2 surface, making UB3LYP a suitable method for geometry optimization of the stationary points along the one-bond cleavage pathway.

As for the question of whether to use DFT or CASSCF to optimize the geometries of stationary points in the decomposition of azoalkanes, UB3LYP and (4,4)CASSCF tend to show good agreement for both the one-bond and the two-bond cleavage pathways, and in the cases of the parent **DBO**, **2**, and **DBH**, both CASPT2//UB3LYP and CASPT2//((4,4)CASSCF) predict the two-bond cleavage to be preferred over one-bond cleavage, although this preference is small in the case of **2**. CASSCF with larger active spaces fails to locate diradical stationary points on the one-bond cleavage pathway and is, therefore, deemed unreliable for the prediction of one-bond versus two-bond cleavage of azoalkanes. CASPT2//CASSCF will provide the correct shape only if the whole reaction path, not just the stationary points from CASSCF, is computed.

Conclusion

Bicyclic azo compounds can decompose by one-bond, two-bond, or three-bond mechanisms, and the “normal” case involves both one-bond and two-bond cleavage occurring simultaneously. Introduction of a fused-cyclopropane or fused-cyclobutane influences both the rate and the preferred mechanism of **DBO** thermal deazetization. Three-bond cleavage is facilitated by pericyclic orbital overlap and is observed when strongly directing Walsh-cyclopropane orbitals are appropriately aligned in exo-cyclopropane **3**. Two-bond cleavage has a very slight enthalpic advantage (ΔH_{0K}^\ddagger) over one-bond cleavage in the absence of a significant stereoelectronic effect, as seen for parent compound **2**, exo-cyclobutane **6**, and endo-cyclobutane **7**. One-bond cleavage is favored when the diazenyl diradical can be significantly stabilized, as is exemplified by the endo-cyclopropane systems, **4** and **5**. However, the one-bond cleavage pathway enjoys an entropic advantage over the two-bond

pathway; consequently, at elevated experimental temperatures, one-bond and two-bond diradical cleavages operate competitively for all compounds except **3** (exclusively three-bond) and **4** (exclusively one-bond).

Acknowledgment. We are grateful to the National Science Foundation for financial support of this research through a research grant to K.N.H. and a graduate fellowship to K.S.K. We also thank the National Computational Science Alliance under grant MCA93S015N and the UCLA Office of Academic Computing for computational resources. K.N.H. acknowledges the stimulating effect of a question from Prof. Jerome Berson from the back of a taxicab in New Haven in January of 1968:

“What do you think causes that inversion in Wolfgang Roth’s bicyclo[2.2.1]azo compound?”

Supporting Information Available: (U)B3LYP/6-31G(d) and Cartesian coordinates and total energies, zero-point vibrational energies and entropies for all stationary points. CASSCF/6-31G(d) coordinates and energies for *trans*-azomethane. CASPT2 electronic energies for select stationary points (PDF). This material is available free of charge via the Internet at <http://pubs.acs.org>.

JA038198L